

Utility of osteon circularity for determining species and interpreting load history in primates and nonprimates

Kendra E. Keenan¹ | Chad S. Mears¹ | John G. Skedros^{1,2}

¹Bone and Joint Research Laboratory,
George E. Whalen Veteran's Affairs Medical
Center, Salt Lake City, Utah

²Department of Orthopaedics, University of
Utah, Salt Lake City, Utah 84132

Correspondence

John G. Skedros, M.D., 5323 South
Woodrow Street, Suite 200, Salt Lake City,
UT 84107, USA.

Email: jskedrosmd@uosmd.com

Abstract

Objectives: Histomorphological analyses of bones are used to estimate an individual's chronological age, interpret a bone's load history, and differentiate species. Among various histomorphological characteristics that can influence mechanical properties of cortical bone, secondary osteon (Haversian system) population density and predominant collagen fiber orientation are particularly important. Cross-sectional shape characteristics of secondary osteons (On.Cr = osteon circularity, On.El = osteon ellipticity) are considered helpful in these contexts, but more robust proof is needed. We sought to determine if variations in osteon shape characteristics are sufficient for accurately differentiating species, load-complexity categories, and regional habitual strain-mode distributions (e.g., tension vs. compression regions).

Materials and Methods: Circularly polarized light images were obtained from 100-micron transverse sections from diaphyses of adult deer calcanei; sheep calcanei, radii, and tibiae; equine calcanei, radii, and third metacarpals (MC3s); chimpanzee femora; and human femora and fibulae. Osteon cross-sectional area (On.Ar), On.Cr, and On.El were quantified indiscriminately and in the contexts of load-complexity and regional strain-mode distributions.

Results: On.Cr and On.El, when examined independently in terms of all data, or mean (nested) data, for each bone, exceeded 80% accuracy in the inter-species comparisons only with respect to distinguishing humans from nonhumans. Correct classification among the nonhuman species was <70%. When On.Cr and On.El were coupled together and with On.Ar in discriminant function analyses (nested and unnested data) there were high misclassifications in all but human vs. nonhuman comparisons.

Discussion: Frequent misclassifications in nonhuman comparisons might reflect influences of habitual load complexity and/or strain-mode distributions, or other factors not accounted for by these two considerations.

KEYWORDS

bone, bone adaptation, haversian system, osteon area, osteon circularity

1 | INTRODUCTION

Physical anthropologists often use histomorphological analyses of skeletal elements (usually limb bone diaphyses) as a means for estimating an individual's chronological age, interpreting a bone's load history, or differentiating species (Brits et al., 2014; Crescimanno and Stout, 2012; Dominguez and Crowder, 2012; Drapeau and Streeter, 2006; Martiniaková et al., 2006; Mulhern and Ubelaker, 2012; Paral et al., 2007; Schaffler and Burr, 1984; Skedros, 2012; Stout and Paine, 1992;

Streeter et al., 2010; Urbanová and Novotný, 2005). Among various histomorphological characteristics of cortical (compact) bone that can influence its mechanical properties, secondary osteon (Haversian system) population density (On.N/T.Ar)¹ and predominant collagen fiber orientation (CFO) are particularly important (Launey et al., 2010; Martin et al., 1998; Riggs et al., 1993b; Skedros, 2012; Skedros et al., 2006, 2013a; Yeni et al., 1997). In contrast to On.N/T.Ar and many other compositional or microstructural characteristics (Table 1), regional variations in predominant CFO across a bone's diaphysis are the strongest

TABLE 1 Summary of a bone's histomorphological characteristics that have been investigated in the context of interpreting load history (Modified from "Interpreting load history in limb-bone diaphyses: Important considerations and their biomechanical foundations," by J. G. Skedros, 2012, *Bone Histology: An Anthropological Perspective*). Biomechanically Important Structural and Material Characteristics in Diaphyseal Bone Hierarchical Organization.

1. Structural characteristics
Bone length
Diaphyseal Curvature
Cross-sectional shape and robusticity [e.g., moments and axes of area (inertia)]
Average and regional cortical thickness variations
2. Material characteristics
Mineral content (% ash)
2a. Microstructure
Secondary osteon population density and fractional area (On.N/T.Ar, On.Ar/T.Ar);
Secondary osteon cross-sectional area (On.Ar), shape (On.Cr), and orientation
Secondary osteon morphotypes (e.g., bright, alternating, parallel-fibered, hooped)
Mineral heterogeneity (e.g., relatively highly mineralized interstitial bone, young osteons, etc.)
Collagen fiber heterogeneity
Porosity (e.g., Haversian canals, primary vascular canals)
Lamellar organization of various osteon morphotypes
Variations in primary histologic organization (e.g., laminar vs. reticular vascular patterns in fibrolamellar/plexiform bone)
Osteocyte and lacunar population density, osteocyte lacuna-canalicular geometries
2b. Nanostructure
Predominant CFO, collagen density
Types and densities of collagen molecular cross-links
Mineral crystallite orientation, size, and heterogeneity
Spatial distribution of noncollagenous proteins (e.g., osteopontin and osteocalcin)

Cancellous (trabecular) bone is not considered here.

predictors of a history of habitual, typically unidirectional, bending (Skedros, 2012; Skedros et al., 2011a). This is because predominant CFO is strongly correlated with strain mode²: relatively longitudinal CFO in habitually tension-loaded regions ("tension regions") and relatively oblique-to-transverse in habitually compression-loaded regions ("compression regions"; Skedros et al., 2009, 2013a). This relationship is important and broadly applicable in studies of bone adaptation because: (1) relatively unidirectional bending (producing prevalent/predominant tension vs. compression on opposite sides of the bone) is highly conserved in many human and nonhuman appendicular long

bone diaphyses, and (2) bending produces the majority (>70%) of longitudinal strains occurring during peak loading of controlled in vivo activity in most limb bones that have been studied, but few of these have been bones from primates (Biewener and Bertram, 1993; Biewener et al., 1986; Demes et al., 1998, 2001; Lieberman et al., 2003; Moreno et al., 2008; Rubin and Lanyon, 1984; Skedros, 2012).

Due to more complex loading, many limb bones experience substantial torsion, which produces prevalent/predominant and diffusely distributed shear strains. This differs from a bone that experiences comparatively unidirectional bending, where the "tension region" and "compression region" are separated by a "neutral axis region" where shear strains are increased and more localized (Demes, 2007). It has been argued that the relatively more uniformly distributed prevalent/predominant shear strains in bones with prevalent torsional loading require preferential tissue-level adaptation (Skedros, 2012) even though coexisting bending can be sufficient to produce "tension regions" and "compression regions" in these bones (Lanyon and Bourn, 1979). This preferential adaptation for shear strains has been called the "shear resistance-priority hypothesis," which is based on the relatively deficient mechanical properties of bone loaded in shear when compared with tension and compression (Skedros, 2012; Skedros et al., 2015). It has been argued that this is the reason why in bones that are habitually torsionally loaded the relationships of CFO and other histomorphological characteristics are less clear with respect to load history even when unidirectional bending coexists (Rubin et al., 2013; Skedros, 2012). In other words, the shear-related histomorphological adaptations in these bones do not exhibit the more obvious marked regional variations in the matrix ultrastructural anisotropy (e.g., predominant CFO) seen in bones that receive habitual bending. This is an important consideration; attempts at correlating load history with regional variations in histomorphological characteristics (i.e., between regions of the same cross-section) may be unsuccessful if it is anticipated that unidirectional bending is sufficient for evoking regional differences in matrix adaptations when the habitual loading is actually much more complex (i.e., shear strains are prevalent and diffusely distributed; **Figure 1**; Goldman et al., 2003; Havill et al., 2013; Mayya et al., 2013; Skedros, 2012; Skedros et al., 2015). In this context, it is notable that "high-complexity" best characterizes the load histories of the regions of limb bones that are typically evaluated in anthropological studies of cortical bone histomorphology (Burr et al., 1990; Carando et al., 1989; Cooper et al., 2007; Demes et al., 2001; Feik et al. 1996; Havill, 2004; Havill et al., 2013; Hillier and Bell, 2007; Martiniaková et al., 2006; Miszkiewicz, 2016; Mulhern and Van Gerven, 1997; Paine and Godfrey, 1997; Pfeiffer et al., 2006; Portigliatti et al., 1984; Schaffler and Burr, 1984; Sinclair et al., 2013; Skedros et al., 2015; Urbanová and Novotný, 2005; Warsaw, 2008).

Additional histomorphological characteristics that are also considered important in terms of adapting the diaphysis of a bone for its load history include secondary osteon collagen/lamellar "morphotypes" (Beraudi et al., 2010; Bigley et al., 2006; Martin et al., 1996; Skedros et al., 2009, 2011a, 2013a), osteon cross-sectional area and diameter (i.e., the "size" of individual osteons; Moyle and Bowden, 1984;

Habitual Load-Complexity Categories Based on N.A. Rotation Criterion	
Complexity Category	Examples
<i>(Based on N.A. rotation during middle portion of typical load phase.)</i>	
<p>Low (N.A.: <10° rotation) (Tension and compression minimally overlap; Shear is localized near N.A.)</p>	<p>1. artiodactyl and perissodactyl calcanei (Lanyon, 1974; Su et al., 1999; Skedros et al., 2016)</p> <p>2. potoroo calcaneus (Biewener et al., 1996)</p> <p>3. chicken metatarsus (Judex et al., 1997; Skedros et al., 2003a)</p>
<p>Moderate A (N.A.: 10° - 20° rotation)</p>	<p>4. dog, sheep and horse radii (Carter et al., 1980; Lanyon et al., 1982; Coleman et al., 2002)</p> <p>5. macaque ulna (Demes et al., 1998; Skedros et al., 2003a)</p>
<p>Moderate B (N.A.: 20° - 40° rotation)</p>	<p>6. human fibula (Lambert, 1971; Thomas et al., 1995; Weaver and Skedros, 2016)</p> <p>7. sheep metatarsal (Lieberman et al., 2004)</p> <p>8. chimpanzee femoral neck (Kalmey and Lovejoy, 2002; Skedros et al., 2008)</p> <p>9. immature turkey ulna (Skedros and Hunt, 2004)</p> <p>10. horse third metacarpal (Gross et al., 1992; Skedros et al., 1996)</p> <p>11. human tibia (Lanyon et al., 1975; Burr et al., 1996; Milgrom et al., 2000; Peterman et al., 2001)</p> <p>12. human femur proximal diaphysis (Skedros et al., 1999; Skedros et al., 2012)</p>
<p>High (N.A.: >40° rotation) (Tension and compression overlap extensively; Shear is relatively more diffusely distributed across the cortex when compared to other categories.)</p>	<p>13. goat radius (Main and Biewener, 2004; Main, 2007; Moreno et al., 2008)</p> <p>14. mature turkey ulna (Rubin and Lanyon, 1985; Skedros and Hunt, 2004)</p> <p>15. horse third metacarpal (Skedros et al., 2006; Rubin et al., 2013)</p> <p>16. human tibia (in some athletes) (Lanyon et al., 1975; Burr et al., 1996; Milgrom et al., 2000; Peterman et al., 2001)</p> <p>17. human femur mid-diaphysis (Cristofolini et al., 1996; Goldman et al., 2003; Drapeau and Streefer, 2006)</p> <p>18. sheep tibia (Lanyon and Bourn, 1979; Lieberman et al., 2004)</p> <p>19. pigeon humerus (Biewener and Dial, 1995)</p> <p>20. chimpanzee femoral neck (Kalmey and Lovejoy 2002; Skedros et al., 2008)</p> <p>21. human femoral neck (Pidaparti and Turner, 1997; Skedros et al., 1999; Skedros and Baucom, 2007)</p> <p>22. free-flying bat humerus (Swartz et al., 1992)</p> <p>23. chicken femur (Carrano and Biewener, 1999; Skedros, 2002)</p> <p>24. alligator femur (Blob and Biewener, 1999; Lee, 2004)</p> <p>25. greyhound femur (Szivek et al., 1992)</p>

FIGURE 1 Load-Complexity Categories (modified from Skedros, 2012). This scheme is based on data from various sources (Biewener and Dial, 1995; Biewener et al., 1996; Blob and Biewener, 1999; Burr et al., 1996; Carrano and Biewener, 1999; Carter et al., 1980; Coleman et al., 2002; Cristofolini et al., 1996; Demes et al., 1998; Drapeau and Streefer, 2006; Goldman et al., 2003; Gross et al., 1992; Judex et al., 1997; Kalmey and Lovejoy, 2002; Lambert, 1971; Lanyon, 1974; Lanyon and Bourn, 1979; Lanyon et al., 1975, 1982; Lee, 2004; Lieberman et al., 2004; Main, 2007; Main and Biewener, 2004; Milgrom et al., 2000; Moreno et al., 2008; Peterman et al., 2001; Pidaparti and Turner, 1997; Rubin and Lanyon, 1985; Rubin et al., 1996, 2013; Ruff et al., 2006; Skedros, 2002; Skedros and Baucom, 2007; Skedros and Hunt 2004; Skedros et al., 1996, 1999, 2003a, 2006, 2008, 2012; Su et al., 1999; Swartz et al., 1992; Szivek et al., 1992; Thomas et al., 1995; Turner, 1998; Weaver and Skedros, 2016)

Moyle et al., 1978; Skedros et al., 2013a; van Oers et al., 2008), and the amount of cement line interfaces, which can be expressed as the percentage of secondary osteonal bone (On.B.Ar/T.Ar; Evans and

Riola, 1970; Gibson et al., 2006; Mayya et al., 2013; Mohsin et al., 2006; Yeni et al., 1997). In studies that have sought to estimate chronological age or classify fragmentary or complete limb bones

into their correct taxa, some of these osteonal characteristics along with several others have been used: for example, (1) Haversian canal area, perimeter, and maximum and minimum diameter, (2) osteon area, perimeter, and maximum and minimum diameter, (3) maximum and minimum diameter ratios of osteons and of Haversian canals, and (4) On.N/T.Ar (Cattaneo et al., 1999, 2009; Hillier and Bell, 2007; Martiniaková et al., 2006; Urbanová and Novotný, 2005). Correct species classification has been achieved 100% of the time in two studies that used predictive equations which incorporated several characteristics: (1) Urbanová and Novotný (2005) incorporated cortical thickness, maximum osteon diameter, and maximum diameter and area of the Haversian canals, and (2) Cattaneo et al. (1999) incorporated maximum and minimum diameter and area of Haversian canals. By contrast, studies that have focused on species differentiation based on differences in limb bone histomorphological characteristics have had less success, with accuracy ranging from 40 to 80% (Cattaneo et al., 2009; Hillier and Bell, 2007; Martiniaková et al., 2006).

The cross-sectional shape of secondary osteons is a characteristic that might be helpful in one or more of these contexts, but has received little attention. Prior studies of osteon shape are mostly theses and abstracts, with some only reporting qualitative observations. These studies considered osteon shape in terms of animal aging, species differentiation, and functional adaptation associated with load history differences between and within bone “types” (e.g., radius vs. calcaneus, femur vs. humerus; Beckstrom, 2010; Britz et al., 2009; Currey, 1964; Dominguez and Crowder, 2012; Goliath et al., 2016; Skedros, 2000; Skedros et al., 2007b; Sorenson et al., 2004; Tersigni et al., 2008; Tersigni-Tarrant et al., 2011). Osteon circularity (On.Cr) can be expressed as a unitless measurement from zero to one (perfect circle = 1):

$$\text{Circularity} = 4\pi \left(\frac{\text{area}}{\text{perimeter}^2} \right)$$

(Britz et al., 2009; Crescimanno and Stout, 2012; Dominguez and Crowder, 2012; Skedros, 2000).

Tersigni and coworkers (Tersigni et al., 2008; Tersigni-Tarrant et al., 2011) report that osteons are more circular in nonhuman limb bones when compared to more elliptical osteons in human limb bones, suggesting the possibility that On.Cr could be useful in differentiating species. However, their work has only been reported in two abstracts that provide very little information. In contrast, Dominguez and Crowder (2012), in a well described analysis, examined the use of On.Cr and/or the area of individual secondary osteons (On.Ar) to distinguish bones from modern humans (ribs only; age range: 16–87 years old) and immature and mature white-tail deer and dogs (humeri, femora, and ribs). Using On.Cr averaged for each bone, they correctly differentiated these three species 66% of the time and correctly differentiated human from non-human bones 76% of the time. When they used both On.Cr and On.Ar averaged for each bone and examined in terms of a discriminant function analysis (DFA), the three species were correctly differentiated about 90% of the time and humans were correctly differentiated from nonhumans 100% of the time. They also showed that osteons in

their specimens tended to be more circular in humans compared to the other species that they examined (based on mean On.Cr (m.On.Cr): human = 0.90, dog = 0.89, deer = 0.88). In contrast, in another well described study, Crescimanno and Stout (2012) found that osteons are typically more circular in the nonhuman bones that they examined, which is similar to the findings reported by Tersigni and coworkers. Their study examined femora, humeri, and ribs from 14 modern humans (54–78 years old; 7 male, 7 female) and from mature pigs, dogs, and white-tail deer. When using On.Cr averaged for each bone (m.On.Cr) they were able to distinguish human from nonhuman bones 76.5% of the time; but the difference in m.On.Cr was also minor, on the order of 2% (0.85 for humans vs. 0.87 for nonhumans).

The contradictory findings between these two well described studies (Crescimanno and Stout, 2012; Dominguez and Crowder, 2012) reduces confidence in the ability of On.Cr (or m.On.Cr) to distinguish human from nonhuman species; the type of human bones used (ribs vs. ribs and long bones) raises the question of alternative causes for variations of osteon circularity within a single species. We could not locate any studies that considered if using these osteon circularity metrics in species differentiation can be confounded by the possibility that bones from different anatomical locations and/or species might also have marked histomorphological variations that are a function of their: (1) prevalent/predominant strain-mode distributions produced by their load history; for example, habitual bending where there are generally mutually exclusive “tension regions,” “compression regions,” and “shear (neutral axis) regions” and (2) load-complexity “category” (in ascending order: low, moderate A, moderate B, and high), where “tension regions” and “compression regions” become less distinct and shear strains become more prevalent and diffusely distributed as load complexity increases (Skedros, 2012; Skedros et al., 2015; Figure 1). Dominguez and Crowder (2012) examined anatomical quadrants, but their study did not extend to consider these in terms of variations in load history that might exist between regions of the cross-sections that they did or did not analyze. Finally, it is not known if On.Cr and On.N/T.Ar are closely related. This is important because, as suggested by Dominguez and Crowder (2012), local variations in On.N/T.Ar might influence On.Cr (e.g., osteons might become more circular as osteon population density increases; Britz et al., 2009). Additional analyses are needed to examine all of these considerations.

The use of ribs as the only primate in an analysis of On.Cr (Dominguez and Crowder, 2012) potentially confounds attempts to differentiate species for various reasons including differences in metabolism and/or adaptability of the axial versus appendicular skeleton (Dominguez and Agnew, 2016; Skedros et al., 2013b). Incorporating the study of human long bones, such as the femur (Crescimanno and Stout, 2012) and additional “control bones” that are subjected to simple bending (e.g., sheep, deer, and equine calcanei and radii) (Sinclair et al., 2013; Skedros et al., 2009), would be beneficial for exploring the use of On.Cr in these comparative contexts. Using bone “types” that represent various load-complexity categories is also essential for determining if this issue could confound species differentiation. Expanding the load histories and “types” of the bones studied is also important for

two additional reasons. First, anthropological studies focusing on species differentiation often do not include bones of the lower-complexity load categories (Hillier and Bell, 2007) where regional histomorphological heterogeneity would more likely confound species differentiation when compared to high-complexity loaded bones (Skedros, 2012; Skedros et al., 2015). The second reason is that of the three nonhuman species examined by Dominguez and Crowder (2012; deer and dogs) and Crescimanno and Stout (2012; deer, dogs, and pigs), deer and dogs are, when compared with the dozens of small and large mammalian species previously studied, are some of the most readily distinguishable from human bones based on relatively simple osteon measurements and/or histological observations (e.g., the predominance of fibrolamellar vs. secondary osteonal bone; Hillier and Bell, 2007).

This study seeks to address many of these issues and possibilities by determining: (1) if variations in On.Cr are, independent of other histomorphological characteristics, sufficient for accurately differentiating species, load-complexity categories, and/or regional habitual strain-mode distributions, (2) if variations in On.Cr that are correlated with bones from mammalian species representing all of the load-complexity categories (Figure 1) and/or if the regional strain-mode distributions in cross-sections of these bones can reduce the accuracy in differentiating species, and (3) if there are important relationships between On.Cr and On.Ar (secondary osteon area), On.N/T.Ar (secondary osteon population density), and On.B.Ar/T.Ar (the fractional area of secondary osteonal bone, including complete osteons and osteon fragments) that might explain variations in On.Cr. Additionally, we examined the degree to which an osteon fits an ellipse (On.El) in these various contexts because this characteristic, though in part accounted for by On.Cr, can be more specific in reflecting functional adaptation in some contexts that is not revealed by the relatively more generic/composite information provided by On.Cr (Hennig et al., 2015). Diagrammatic examples of regional On.Cr and On.El variations expected within and between bones subject to habitual torsional loading vs. habitual typically unidirectional bending are shown in Figure 2.

2 | METHODS

2.1 | Specimens

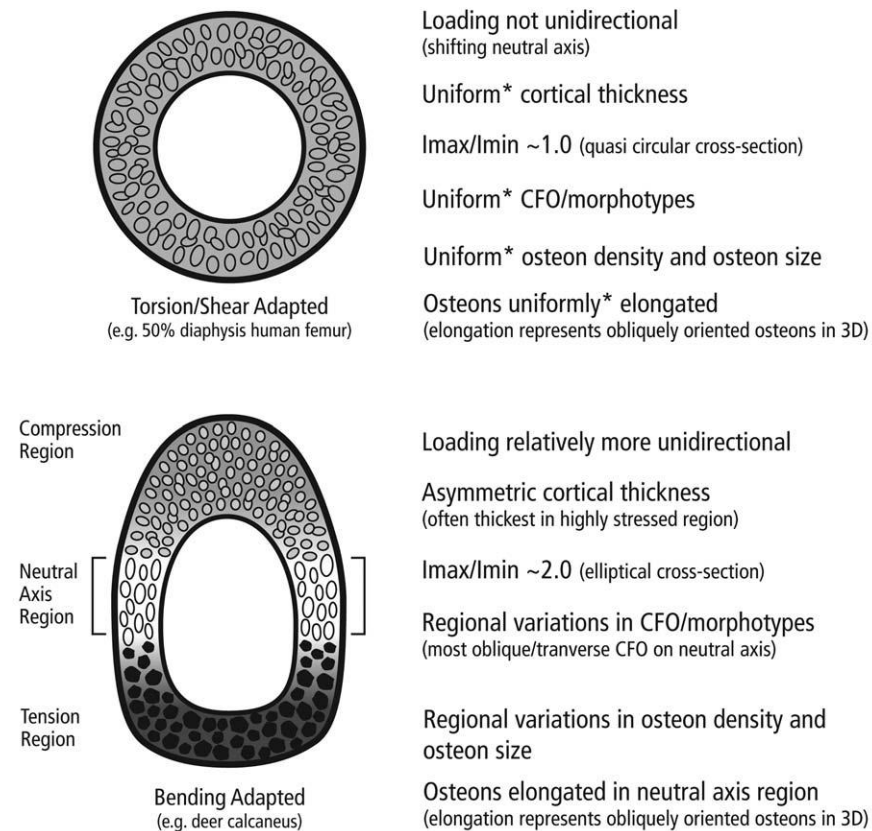
The histomorphometric methods used in this study have been described previously (Skedros et al., 2009, 2011a). Briefly, circular polarized light (CPL) microscopic images of all the unstained/undecalcified bones used herein were obtained at 50 \times from thin ultramilled/polished (100 μ m) transverse sections. Most of the histomorphological data not dealing with osteon cross-sectional shape that are reported herein are from our previous studies that used the following samples of bones from skeletally mature animals: (1) Rocky Mountain mule deer calcanei ($n = 7$), (2) sheep calcanei, radii, and tibiae ($n = 7$ each bone "type"), (3) equine calcanei, radii, and third metacarpals (MC3s; $n = 7$ each bone "type"; Skedros et al., 2009), (4) chimpanzee femora ($n = 8$; mean age 25 years; age range: 18–31 years; 3 males; 4 females; one unknown sex; Beckstrom, 2010; Skedros et al., 2011a), and (5) modern human femora ($n = 12$; mean age: 53; age range: 22–71 years; 3 males;

9 females; Skedros et al. 1999, 2012). Modern human fibulae ($n = 11$; mean age: 47; age range: 25–65 years; 8 males; 3 females) were also used and the data from these bones have not been published. All individuals in all human and nonhuman samples were healthy prior to death, had no evidence of musculoskeletal disease, and had not taken medications that could alter bone metabolism or remodeling activity. As shown in our prior studies, we typically analyzed at least 80% of the middle of the central cortex in cortical quadrants (most bones) or octants (human and chimpanzee femora) to sufficiently account for local variation (Iwaniec et al., 1998) and our specimens are sufficiently powered for discerning differences in load history.

2.2 | Procedures

In the bones that typically experience habitual relatively unidirectional bending, CPL images were taken in locations that experience prevalent/predominant tension, compression, or shear (neutral axis; Skedros et al., 2009). As described by Skedros (2012), these bones are naturally subject to loading that spans a range from relatively simple bending to bending coexisting with increased prevalence of torsion during typical peak ambulatory activities (Figure 2). Load-complexity categories were as follows: (1) "low-complexity" includes sheep, deer, and equine calcanei, (2) "moderate-A complexity" includes sheep and equine radii, and (3) "moderate-B complexity," defined as bending with relatively increased torsion during habitual loading, includes equine MC3s, human fibulae, and chimpanzee and human femora. The load-complexity category of the mid-to-distal diaphysis of the human fibula was not considered in Skedros (2012). For this study, our rationale for designating the adult human fibula in the "moderate-B complexity load category" is based on: (1) a literature review (Weaver and Skedros, 2016) that examined analytical and strain data from prior studies [including Lambert (1971) and Thomas et al. (1995)], and (2) studies of patterns of predominant CFO that relate to prevalent/predominant strain mode in transverse sections from the mid-to-distal diaphysis of adult bones (Carando et al., 1989; Skedros and Keenan, 2016). Finally, the sheep tibiae are the only bones analyzed in this study that are from the "high-complexity load category," these bones have the greatest habitual torsional loading in addition to some bending (Lanyon and Bourn, 1979; Skedros et al., 2009). To maintain adequate sample sizes for the statistical analyses (described below), the "moderate-A complexity load category" and the "moderate-B complexity load category" are combined into one "moderate-complexity load category," which is reflected in a majority of the tables and figures. As mentioned above, there is the least amount of load-induced variation in location of the neutral axis in the "low-complexity load category," and the most variability of the location of the neutral axis is in the "high-complexity load category." Because of this broadly shifting neutral axis in the sheep tibia ("high-complexity load category"), the designation of "strain-mode locations" is not applicable for this bone (Figures 1 and 2 top drawing). Additional discussion of the rationale used to designate load-complexity categories and the histomorphological variations that might help to distinguish them can be found in Skedros (2012).

Expected Osteon Characteristics and Bone Geometry



*Quasi "uniformity" (not strict uniformity) is seen in actual highly torsionally loaded bones

FIGURE 2 Cross-sections of bones that are habitually loaded in prevalent torsion (top) and bending (bottom). The secondary osteons are shown in a stylized manner as based on data or observations reported previously. For the top drawing, the osteons are shown as ellipses as would be expected in terms of the highly oblique 3D orientations observed by Petrtyl et al. (1996) in epifluorescent images of India ink-stained longitudinal sections of mid-diaphyseal femora of modern humans. The osteons in the bottom drawing are based on observations of Skedros et al. (Skedros et al., 1994, 2007b), which resemble those shown in Figure 3 of this study. At the right of each section are descriptions of the general differences between the top and bottom sections (I = second moment of area; I_{max}/I_{min} provides an index of cross-sectional shape). As noted in the more torsionally loaded bones, "uniform" means "reduced regional variations" when compared with the more simply/unidirectionally loaded bones

The nonprimate bones and human fibulae were examined in the superior (proximal) aspect of the middle one-third of the diaphysis. The human and chimpanzee femora were analyzed in the proximal diaphysis (subtrochanteric region) where the bending moment is high and torsional stress is moderate (Skedros and Baucom, 2007; Skedros et al., 2013a). Secondary osteon population density (On.N/T.Ar), fractional area of secondary osteon bone (On.B.Ar/T.Ar, expressed as a percentage), and the cross-sectional area of individual secondary osteons (On.Ar) were quantified for each digitized image in our previous studies (Skedros et al., 2009, 2011a, 2012, 2013a). In most cases the On.Cr data were also obtained in these prior studies, but they were not reported in the published studies. On.B.Ar/T.Ar data were not obtained from the human femora or human fibulae and On.Ar data were not obtained from the chimpanzee femora.

ImageJ [v. 1.43, National Institutes of Health, USA (Rasband, 1997–2016)] was used to obtain the osteon circularity (On.Cr), osteon

ellipticity (On.El), and other histomorphological data that had not been previously obtained. For the nonprimate specimens, all of the complete secondary osteons in each CPL image were analyzed due to their relatively smaller sample size. For the primate specimens, five osteons were randomly selected from each image for On.Cr and On.El analysis. Each osteon was randomly selected using a grid system. Rarely, there were fewer than five secondary osteons in an image; in these cases all quantifiable osteons in the image were measured. Only complete secondary osteons with clearly defined reversal lines (cement lines) and intact Haversian canals were included in our analysis. We examined ~5,000 total osteons of type I and II as described by Skedros et al. (2007b) and Crescimanno and Stout (2012) across all species and bone types in this study. We also considered, but purposefully did not employ, the osteon selection criteria of Dominguez and Crowder (2012), and Crescimanno and Stout (2012). These investigators eliminated osteons with noncircular canals [i.e., central (Haversian) canals of

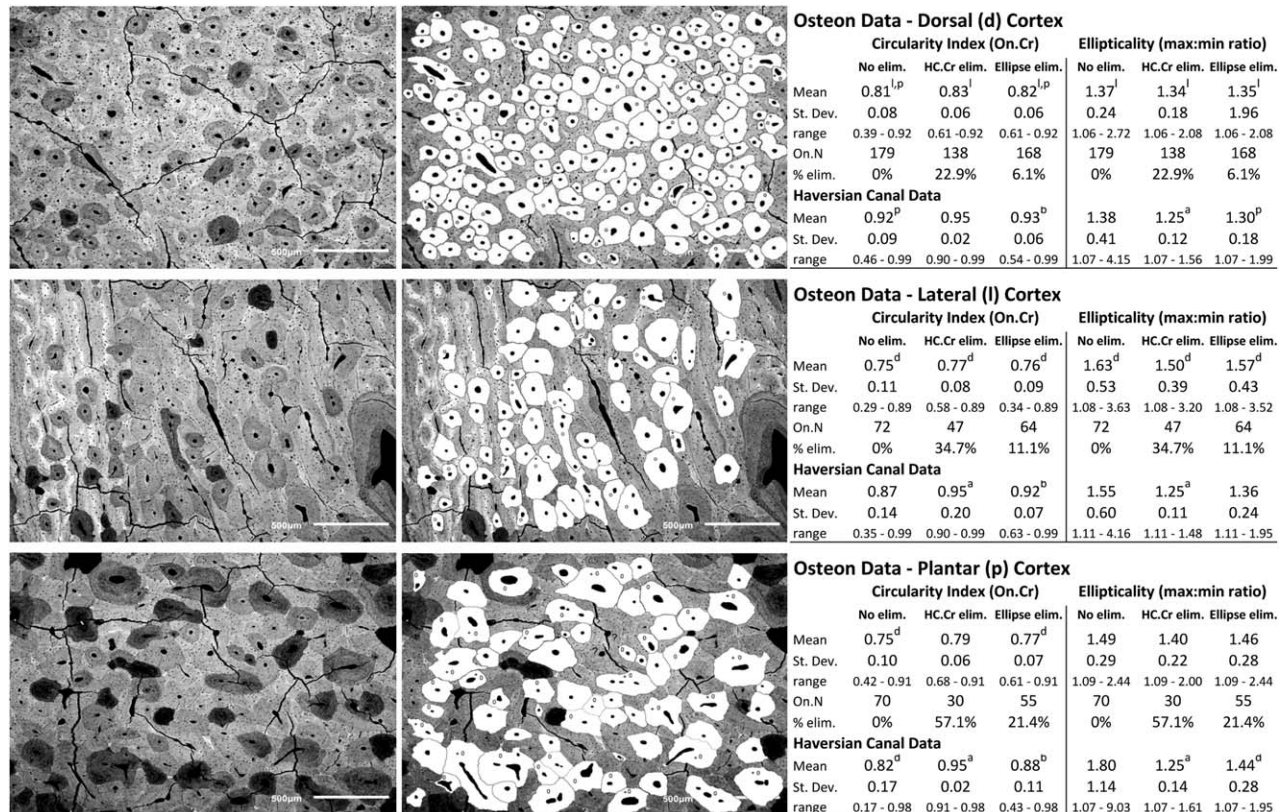


FIGURE 3 (a) Backscattered electron images from the dorsal “compression” (at top), lateral “neutral” axis (middle), and plantar “tension” (at bottom) cortices of a skeletally mature mule deer calcaneus. (b) The osteons that are traced for shape analysis are shown in white, and those marked with a “o” would have been eliminated had we used the HC.Cr (Haversian canal circularity) criteria of Dominguez and Crowder (2012) and those marked with a “+” would have been eliminated had we used the “ellipticity” criteria of Crescimanno and Stout (2012). (c) The differences shown at the far right are those with no eliminations and with eliminations. **St. Dev.** = standard deviation, **On.N** = number of complete secondary osteons, **elim.** = elimination. Paired t-tests were run to estimate the potential statistical significance of the differences. The superscripts represent: **a**: significantly different from no elimination (only applicable to the same region). **b**: significantly different from On.Cr (only applicable to the same region). **d**: significantly different from dorsal “compression” cortex. **l**: significantly different from lateral cortex. **p**: significantly different from plantar “tension” cortex

the secondary osteons]. We did not use these selection criteria because they might bias our various analyses by eliminating osteons that should be selected in cases where variations of On.Cr and On.El are considered adaptations for differences in load history (Mears et al., 2014; Skedros et al., 2013a, 2014a). Here, it is important to emphasize that in the absence of a 3D analysis, it is not known if the elimination criteria of Dominguez and Crowder (2012) and Crescimanno and Stout (2012; these studies focus on species determination) eliminate osteons coursing significantly oblique to the long axis of the bone diaphysis or eliminate less circular or other unusually shaped osteons that are independent of osteon obliquity in 3D (Hennig et al., 2015). In either case, the eliminated osteons can be important in enhancing mechanical toughness in several of the bones studied herein (Skedros et al., 2013a). Therefore, these osteons were not eliminated for the purposes of this study (Figure 3). The only osteons that were excluded from our study were those with dramatic irregularities (e.g., drifting osteons) as described previously (Skedros et al., 2013b), or osteons that were in the process of (or had recently been) resorbed or replaced (Skedros et al., 2007b, 2013b).

Each osteon chosen for quantification was then selected in Adobe Photoshop using the “quick select” tool. Then the “stroke” and “fill” functions were applied to paint each osteon. These images were subsequently opened in ImageJ where each painted osteon was individually selected with the “wand selection” tool and then the “interpolation spline” function was applied to smooth the pixels at the periphery of the osteon, at which point each osteon was then measured. Without this step, extraneous pixels at the osteon periphery would have inadvertently been quantified; if this had occurred it would have artificially and disproportionately reduced On.Cr because the (perimeter)² value is in the denominator of the circularity equation (see above; Mears et al., 2014, 2015). In addition to obtaining On.Cr, On.El was also measured for the same five osteons from each image from the primate and nonprimate bones. On.El is defined as the maximum/minimum chord length of an individual osteon (Skedros et al., 2014a). In these prior studies, we considered the limitations in measurement of On.Cr and have found these methods to be robust to account for such limitations.

2.3 | Statistical analysis

All statistical analyses were done using STATA 14.1 software (Stata-Corp 2015) and included: (1) correlations, (2) analysis of variance (ANOVA), and (3) DFA. Pearson correlation coefficients were used to determine potential relationships between On.Cr, On.El, On.Ar, On.N/T.Ar, and On.B.Ar/T.Ar. These correlation analyses considered osteons from all regions of each bone and from specific cortical regions within each bone. Only unnested (nonmean) data (i.e., all selected osteons) were used in the correlation analyses because: (1) our 2013 study that examined relationships of osteon and central canal areas in 24 samples from eight species did not detect differences between the nested and unnested data until the 100th decimal place (Skedros et al., 2013b) and (2) to avoid spurious correlations when using the small sample sizes resulting from nesting the data. This reasoning was also applied to our ANOVA analysis.

A series of two-way ANOVA were used to evaluate differences in On.Cr and/or On.El for the following: (1) interspecies, (2) intraspecies, (3) load-complexity category, (4) strain-mode distribution (i.e., "tension regions" vs. "compression regions" vs. "neutral-axis regions"), (5) primates vs. nonprimates, and (6) humans vs. nonhumans. We were able to use the ANOVA with Fisher's LSD test in the present study. The paired t-test, which is the post-hoc test for significance following the F test in the ANOVA test, was deemed sufficiently robust for the normality assumption. Furthermore, the Fisher's LSD was chosen for post-hoc analysis because the likelihood of type I errors in the context of a significant test is very low, but without compromising statistical power (Stoddard, 2016 http://medicine.utah.edu/ccts/sdbc/resources/library.php#sdbc_library_stoddard_link).

Linear DFA was used to analyze how accurately species and load-complexity category can be differentiated based on On.Cr, On.El, and On.Ar data independently and when using combinations of these characteristics. This was done similar to the DFA approaches used in prior studies that examined the use of bone histomorphology to distinguish species (Cattaneo et al., 1999, 2009; Dominguez and Crowder, 2012; Martiniaková et al., 2006; Urbanová and Novotný, 2005). In accordance with the methods of Dominguez and Crowder (2012), we performed DFA using all osteon geometric data as independent events (independent/nonmean data; namely, all data for each histological characteristic of interest) and as a mean (quasi-nested) data of each histological characteristic/parameter for each bone. The quasi-nested data were obtained by calculating the mean value for each parameter of each bone within a specimen. In this analysis the mean value represents an independent event. While attempting to account for independence, this substantially reduces the sample size, and therefore it is not truly nested (hence described herein as "quasi nested") as the values were not obtained using a bootstrapping method (Skedros et al., 2013b).

DFA was employed as predictive model to determine how well a given variable, or combination ("+" of variables, correctly classified the specimen and/or category of specimens of interest. This type of analysis resembles that described by Crescimanno and Stout (2012) who used a predictive equation and also by Dominguez and Crowder (2012) who used DFA.

The DFA method of Dominguez and Crowder (2012) was used in this study in terms of determining "percent correct" or, in other words, in quantifying how well the variable in question accurately predicted the specimen's taxonomic or anatomical provenance. In this study, a percent correct <70% was considered insufficient to reliably differentiate specimens, and therefore specific values <70% are usually not reported. Nevertheless, a misclassification occurring in at least 50% of cases was considered pertinent as it shows a high preponderance for potential misinterpretations.

3 | RESULTS

3.1 | Correlations

As expected, On.Cr and On.El are negatively correlated (*r*-values ranging from -0.51 to -0.97 , $p < .05$) and this was consistent in all bones (Table 2). Only three of these 40 comparisons are not statistically significant, which included the cranial cortex of the equine radius, cranial cortex of the sheep tibia, and anterior cortex of the human fibula.

A large majority of the correlations between On.Ar and On.Cr are weak and lack statistical significance. One third of the statistically significant correlations are positive and the remaining are negative; only 30% of all the correlations of On.Ar vs. On.Cr are statistically significant and only 12.5% of the correlations of On.Ar vs. On.El are statistically significant. These results lead to the conclusion that On.Ar does not impact On.Cr or On.El in such a way that could confound results.

As shown in Table 2, correlations are also typically weak between On.N/T.Ar and On.Cr, and between On.N/T.Ar and On.El, and 75% of these comparisons are not statistically significant. Furthermore, (1) only 19% of the correlations of On.B.Ar and On.Cr are significant and only two coefficients are >0.7 , and (2) 11% of the correlations of On.B.Ar/T.Ar and On.El are significant and of the few significant comparisons only one is >0.7 . These results suggest that the On.N/T.Ar and On.B.Ar/T.Ar do not affect osteon shape.

As expected, On.N/T.Ar and On.B.Ar/T.Ar are often strongly and positively correlated (range: $r = 0.30$ – 0.97 , $p < .05$; $r > 0.7$ in 50% of comparisons). This strong relationship is consistent with findings reported in our previous studies that examined many of the same bones (69, 86). In those studies it was determined that variation in osteon size (On.Ar) is the main reason for the weaker correlations of some of the On.N/T.Ar versus On.B.Ar/T.Ar comparisons.

A subset analysis looked at age vs. the following parameters: On.Cr, On.El, and On.Ar in the human femora. There were no statistically significant correlations, or were there even any weak correlations (i.e., the absolute values for the *r*-values range from 0.014 to 0.149).

3.2 | ANOVA and DFA

This section addresses ANOVA and DFA analyses for the following comparisons: (1) interspecies, (2) intraspecies, (3) load-complexity category, (4) strain-mode distributions, (5) primates versus nonprimates, and (6) humans versus nonhumans. For each of these six types of comparisons, the data were analyzed based on all independent data points

TABLE 2 Table of correlation coefficients and corresponding *p* values for all comparisons

	On.N/T.Ar vs. On.Cr.	On.N/T.Ar vs. On.B.Ar/T.Ar ^a	On.N/T.Ar vs. On.El	On.Cr. Vs. On.B.Ar/T.Ar ^a	On.Cr. vs. On.El	On.B.Ar/T.Ar vs. On.El ^a	On.Ar vs. On.Cr ^a	On.Ar vs. On.El ^a
All Osteons	0.43 (<0.001)	0.57 (<0.001)	NS	NS	-0.54 (<0.001)	NS	0.42 (<0.001)	0.08 (0.02)
Compression	0.38 (<0.001)	0.33 (<0.001)	NS	NS	-0.56 (<0.001)	NS	0.47 (<0.001)	NS
Tension	0.37 (<0.001)	0.45 (<0.001)	NS	NS	-0.51 (<0.001)	NS	0.35 (<0.001)	NS
Neutral Axis	0.54 (<0.001)	0.70 (<0.001)	NS	NS	-0.59 (<0.001)	NS	0.46 (<0.001)	NS
Sheep Calcaneus	NS	0.76 (<0.001)	NS	NS	-0.90 (<0.001)	NS	NS	NS
Compression	NS	NS	NS	NS	-0.95 (<0.001)	NS	NS	0.66 (0.04)
Tension	NS	NS	NS	NS	-0.90 (<0.001)	NS	NS	0.93 (<0.001)
Neutral Axis	NS	0.81 (<0.001)	NS	NS	-0.93 (<0.001)	NS	-0.87 (0.001)	NS
Deer Calcaneus	NS	0.87 (<0.001)	NS	NS	-0.74 (<0.001)	NS	NS	NS
Compression	NS	NS	NS	-0.67 (0.03)	-0.71 (0.020)	NS	NS	NS
Tension	NS	NS	NS	NS	-0.86 (0.002)	NS	NS	NS
Neutral Axis	NS	0.80 (<0.001)	NS	NS	-0.68 (0.001)	NS	NS	NS
Equine Calcaneus	0.29 (0.03)	0.32 (0.018)	NS	NS	-0.86 (<0.001)	NS	-0.27 (0.05)	NS
Compression	NS	NS	NS	NS	-0.85 (<0.001)	NS	NS	NS
Tension	NS	NS	NS	NS	-0.62 (0.014)	NS	NS	NS
Neutral Axis	NS	0.52 (0.019)	NS	NS	-0.90 (<0.001)	NS	NS	NS
Equine Radius	0.40 (<0.001)	0.86 (<0.001)	-0.38 (<0.001)	0.37 (<0.001)	-0.74 (<0.001)	-0.27 (0.02)	NS	NS
Compression	NS	0.74 (<0.001)	NS	NS	-0.85 (<0.001)	NS	NS	NS
Tension	NS	NS	NS	NS	NS	NS	NS	NS
Neutral Axis	NS	0.91 (<0.001)	NS	NS	-0.79 (<0.001)	NS	NS	NS
Sheep Radius	NS	0.79 (<0.001)	NS	NS	-0.79 (<0.001)	NS	NS	NS
Compression	0.67 (0.03)	0.93 (<0.001)	NS	NS	-0.68 (0.029)	NS	NS	NS
Tension	NS	NS	NS	NS	-0.65 (0.040)	NS	NS	NS
Neutral Axis	NS	0.70 (<0.001)	NS	NS	-0.88 (<0.001)	NS	NS	NS
Equine MC3	0.47 (<0.001)	0.90 (<0.001)	-0.43 (<0.001)	0.44 (<0.001)	-0.91 (<0.001)	-0.40 (<0.001)	-0.31 (0.005)	0.28 (0.01)
Compression	0.75 (<0.001)	0.94 (<0.001)	-0.70 (<0.001)	0.76 (<0.001)	-0.97 (<0.001)	-0.72 (<0.001)	NS	NS
Tension	0.82 (<0.001)	0.94 (<0.001)	-0.67 (0.003)	0.77 (<0.001)	-0.83 (<0.001)	-0.57 (0.01)	NS	NS
Neutral Axis	NS	0.87 (<0.001)	NS	NS	-0.89 (<0.001)	NS	-0.37 (0.02)	NS
Sheep Tibia	NS	0.92 (<0.001)	NS	NS	-0.84 (<0.001)	NS	NS	NS
Compression	NS	0.64 (0.045)	NS	NS	-0.83 (0.003)	NS	NS	NS
Tension	NS	0.97 (0.007)	NS	NS	NS	NS	NS	NS
Neutral Axis	NS	0.93 (<0.001)	NS	NS	-0.79 (0.019)	NS	NS	NS
Chimpanzee Femur	NS	0.30 (<0.001)	NS	0.24 (0.007)	-0.80 (<0.001)	NS	-	-
Compression	NS	0.52 (0.039)	NS	NS	-0.72 (0.002)	NS	-	-
Tension	NS	NS	NS	0.52 (0.04)	-0.81 (<0.001)	NS	-	-
Neutral Axis	NS	0.47 (0.006)	NS	NS	-0.82 (<0.001)	NS	-	-
Human Femur	0.12 (0.04)	-	NS	-	-0.81 (<0.001)	-	-0.34 (<0.001)	NS
Compression	NS	-	NS	-	-0.83 (<0.001)	-	-0.56 (<0.001)	NS

(continues)

TABLE 2 (continued)

	On.N/T.Ar vs. On.Cr.	On.N/T.Ar vs. On.B.Ar/T.Ar ^a	On.N/T.Ar vs. On.El	On.Cr. Vs. On.B.Ar/T.Ar ^a	On.Cr vs. On.El	On.B.Ar/T.Ar vs. On.El ^a	On.Ar vs. On.Cr ^a	On.Ar vs. On.El ^a
Tension	NS	-	NS	-	-0.87 (<0.001)	-	NS	NS
Neutral Axis	NS	-	NS	-	-0.75 (<0.001)	-	NS	NS
Human Fibula	NS	-	-0.25 (0.01)	-	-0.62 (<0.001)	-	-0.29 (0.004)	0.22 (0.04)
Compression	NS	-	-0.45 (0.03)	-	-0.79 (<0.001)	-	NS	NS
Tension	NS	-	NS	-	NS	-	NS	NS
Neutral Axis	NS	-	NS	-	-0.88 (<0.001)	-	-0.30 (0.04)	NS

All values shown are significant at $p < .05$. NS = not significant. Dark grayed cells are correlations where the r -value was 0.7 or greater. Note, the data in the same row as the species and bone name is for all osteons in that category.

^aThere are no osteon area (On.Ar) data for our chimpanzee specimens and no fractional area of secondary bone (On.B.Ar/T.Ar) data for our human specimens, as denoted by the blank cells.

R -values for various correlations.

from all the specimens (i.e., nonmean data). For DFA a mean value was used for each specimen (i.e., quasi nested). For each analysis, DFA was done using: (1) On.Cr, (2) On.El, (3) On.Ar, (4) On.Cr + On.El, (5) On.Cr + On.Ar, (6) On.El + On.Ar, and (7) On.Cr + On.El + On.Ar. The "+" indicates the combination of each of the given parameters, in effect as a new parameter, to classify specimens rather than as an additive effect of the values of each parameter. For example, if using On.Cr + On.Ar in the human versus nonhuman analysis, a specimen may be classified as a human if the On.Ar is greater than a given number and the On.Cr is also greater than a certain number, but it is not the sum of values that represent the On.Cr and On.Ar for that specimen. This is based on the idea that by combining parameters, a more specific inclusion rule can be made to correctly classify a specimen. While in this example this approach may improve the confidence that a specimen is indeed human if each inclusion criteria is met, it also increases the risk that important specimens will be falsely excluded. By using each of the above combinations, potentially spurious over- or under-classifications are less likely to occur. The main results are summarized below.

3.2.1 | Interspecies comparisons: What differences in osteon shape exist between species?

3.2.1.1 | ANOVA

Interspecies ANOVA comparisons of independent (nonmean) On.Cr data show several statistically significant differences (Figure 4). However, as is also shown in Figure 4b,c, the reliability of using On.Cr to differentiate these species is substantially impaired because there are significant On.Cr differences between the different bones within each of the horse, sheep, and human species. Results of two-way ANOVA for On.Cr and On.El can be found in Table 3.

3.2.1.2 | DFA

When considering only nonhuman species, DFA of independent (nonmean) On.Cr data also showed a very limited ability to correctly differentiate among the nonhuman species. Horse was the only nonhuman species with a percent correct >50%, but at best, had a maximum percent correct of only 62%. The use of On.El in this context is even

worse, with <50% correct in the interspecies DFA for On.El + On.Ar for all nonhuman species.

When considering all bones for each species without a distinction for load-complexity category, DFA of independent (nonmean) data for human had a percent correct of 100% for On.Cr, On.Cr + On.Ar, and for On.Cr + On.El + On.Ar, and of 85% for On.El + On.Ar. Deer had a percent correct of 100% for On.Cr + On.Ar and for On.Cr + On.El + On.Ar. Horse had a percent correct of 73% for On.Cr + On.Ar. All other comparisons had a percent correct of <70%.

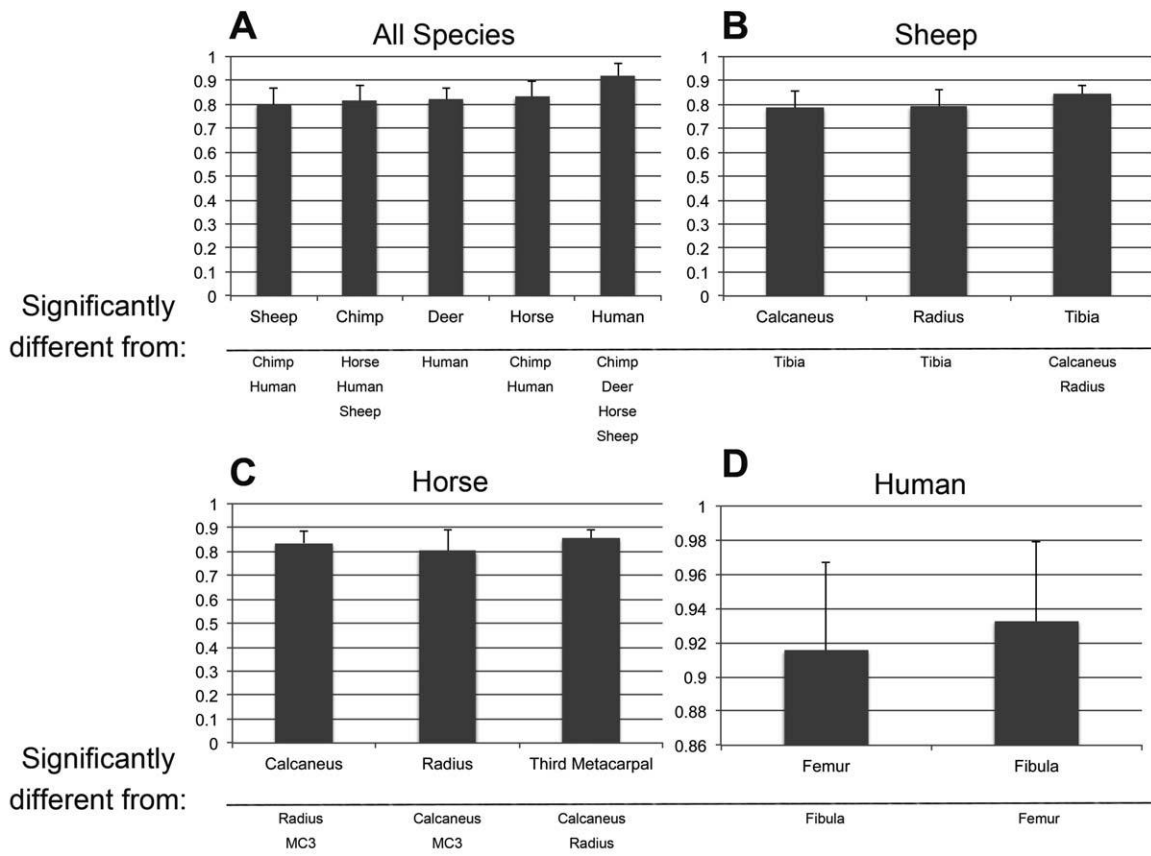
3.2.2 | Intraspecies comparisons: What differences in osteon shape exist within a species?

3.2.2.1 | ANOVA

When using an ANOVA design to look at comparisons of On.Cr and On.El, there are significant differences between the bone "types" within the individual species (e.g., for On.Cr horse radius differs significantly from horse calcaneus). This is shown in Figure 4b-d. Additionally, as in Section 3 of the results and shown in Figure 5 for independent (nonmean) data, there are significant differences in On.Cr stratified by load-complexity category within sheep; however, no statistically significant difference existed for horse. This is the same for all species for independent (nonmean) On.El data. Both human bone types analyzed (fibulae and femora) were classified under moderate-complexity for load-complexity category and therefore were not included in this analysis.

3.2.2.2 | DFA

For the intra-species DFA of independent (nonmean) data from different limb bones, data are available for horse, sheep, and human (Figure 6). Horse included the calcaneus, third metacarpal (MC3), and radius. The MC3 had a percent correct of 75% for On.Cr, 75% for On.Cr + On.El, and 71% for On.Cr + On.Ar. All others had a percent correct of <70%. The sheep included the calcaneus, radius, and tibia. The sheep tibia had a percent correct of 83% for On.Cr + On.El, 81% for On.Cr + On.El + On.Ar, 81% for On.Cr, 80% for On.Cr + On.Ar, 73% for On.Ar + On.El, and 73% for On.Ar. The sheep radius and calcaneus



Note: All listed significant differences are for $p < 0.001$.

FIGURE 4 (a) Bar graphs of interspecies comparisons for On.Cr (mean \pm SD); statistically significant differences are also shown. (b-d) Bar graphs showing statistically significant On.Cr differences between bone types within the same species

TABLE 3 Two-way ANOVA table for On.Cr and On.El showing interactions between variables

On.Cr				On.El			
Factor	Sum of squares	F-ratio	p-value	Factor	Sum of squares	F-ratio	p-value
Ellipticality	3.38	2674.53	<0.001	Circularity	71.03	3096.53	<0.001
Species	0.38	75.58	<0.001	Species	6.51	70.96	<0.001
Ellipticality*species	0.10	201.60	<0.001	Circularity*species	5.43	59.16	<0.001
Ellipticality	7.02	2304.71	<0.001	Circularity	84.84	2365.88	<0.001
Strain mode	0.03	3.28	0.02	Strain mode	3.95	36.73	<0.001
Ellipticality*strain mode	0.01	0.83	0.48	Circularity*strain mode	3.33	30.98	<0.001
Ellipticality	2.86	939.24	<0.001	Circularity	38.86	1088.29	<0.001
Location	0.05	2.37	0.02	Location	4.65	18.60	<0.001
Ellipticality*location	0.02	1.16	0.32	Circularity*Location	3.95	15.80	<0.001
Load-complexity category	0.05	8.26	<0.001	Circularity	8.19	229.10	<0.001
Ellipticality*load-complexity category	0.001	0.24	0.79	Load-complexity category	2.83	39.63	<0.001
				Circularity*load-complexity category	3.58	50.03	<0.001

Dark grayed cells indicate that an interaction is present. The dark grayed cells indicate where there is an interaction present between variables, meaning that one variable has an effect on another variable. An interaction was established to exist for any interaction term with a p -value $< .001$. The interaction term is found in the row with both variable names connected by an asterisk.

TABLE 4 Summary of the main histological characteristics that we have investigated in the context of interpreting load history

	Nonprimates						Primates			
	Simple complexity loads		"Moderate A" complexity loads		"Moderate B" complexity loads		High complexity loads		"Moderate B" complexity loads	
	Sheep calcaneus	Deer calcaneus	Equine calcaneus	Equine radius	Sheep radius	Equine MC3	Equine tibia ^a	Chimp femur	Human femur	Human fibula
Relationships with habitual strain mode?										
Are osteons smaller in "compression" vs. "tension" regions?	Y ^b	Y ^b	Y ^b	N ^b (C > T)	Y ^b	N (C = T)	N (C = T)	Y ^b	N ^b (C > T)	Y ^b
Is osteon population density (On.N/T.Ar) greater in "compression" vs. "tension" regions?	Y ^b	Y ^b	Y ^b	Y ^b	Y ^b	Y ^b	N (C = T)	N (C = T)	N (C = T)	N (C = T)
Is the fractional area of secondary bone (On.B/T.Ar) higher in "compression" vs. "tension" regions?	N ^b (C < T)	N ^b (C < T)	N (C = T)	Y ^b	Y ^b	Y ^b	N ^b (C < T)	N ^b (C < T)	-	-
Are osteons more circular in "compression" vs. "tension" regions?	N (C = T)	Y ^b	Y ^b	Y ^b	N (C = T)	N (C = T)	N (C = T)	N (C = T)	N (C = T)	N (C = T)
Are osteons more circular in "compression" vs. "N.A." regions?	N (C = N.A.)	N (C = N.A.)	Y ^b	N (C = N.A.)	Y ^b	N (C = N.A.)	N (C = N.A.)	N (C = N.A.)	N (C = N.A.)	N (C = N.A.)
Are osteons more elliptical in "N.A." vs. "compression" regions?	N (C = N.A.)	N (C = N.A.)	Y ^b	N (C = N.A.)	Y ^b	N (C = N.A.)	N (C = N.A.)	N (C = N.A.)	N (C = N.A.)	N (C = N.A.)
Is collagen more oblique-to-transverse in "compression" regions?	Y ^b	Y ^b	Y ^b	Y ^b	Y ^b	Y ^b	N ^a (C = T)	Y ^b	Y ^b	ST

Rows 4–6 show results from this study. Rows 1–3 and 7 are from prior studies as summarized in Skedros et al. (2011a).

^aThe sheep tibiae, when compared to the other bones, have "tension" (cranial) versus "compression" (caudal) regions that do not have similar prevalent/predominant tension and compression strain modes, respectively, because habitual torsion produces substantial shear in these regions, which is considered to have a more important effect on adapting the matrix of these regions to functional loads (Skedros 2012).

^bThese comparisons are statistically significant ($p < .05$). C = Compression; T = Tension; Y = Yes; N = No; Empty cell = data not available; N.A. = Neutral axis region (usually high shear region); C = T or C = N.A. denotes no significant difference; S.T. = statistical trend, $p = .08$ (Skedros and Keenan, 2016).

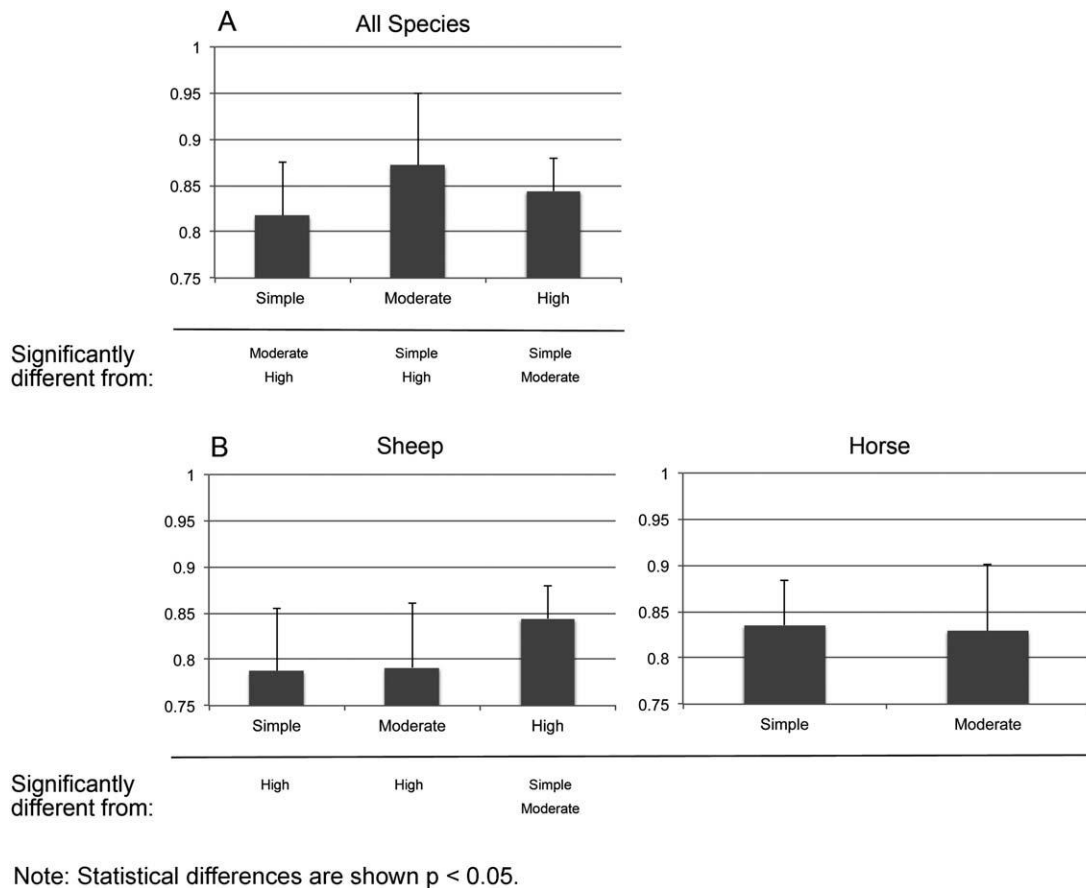


FIGURE 5 (a) Bar graphs showing statistically significant differences in On.Cr (mean \pm SD) in terms of load-complexity category. (b) Statistically significant differences between load-complexity category of the three bones from the sheep and horse

had a percent correct of $<70\%$. The human included the femur and fibula, both of which had a percent correct of $<70\%$.

Data available for intra-species DFA using mean data (quasi-nested) include: horse, sheep, and human, and include the same bones as in the independent (nonmean) analysis. The sheep tibia had a percent correct of 100% for each of the parameters and their combinations with the exception of On.Ar ($<70\%$). The sheep calcaneus also had a percent correct of 100% for On.Cr + On.El + On.Ar, On.Ar + On.Cr, On.Ar + On.El, and On.Ar, but a percent correct of $<70\%$ for the other three parameters. The sheep radius had a percent correct of 80% for On.Cr + On.El + On.Ar, and for On.Cr + On.Ar, but for all the other parameters the percent correct was $<70\%$. When using On.Cr and On.Cr + On.El, the sheep calcaneus was misclassified as a sheep radius in 60% of cases. The human femur had a percent correct of 100% for On.Cr + On.El + On.Ar, 83% for On.Cr + On.El, 75% for On.Cr + On.Ar and for On.Ar, and a percent correct, 70% for the remaining three parameters. The human fibula had a percent correct of 77% for On.Cr + On.El + On.Ar, On.Cr + On.El, On.Ar + On.El, and On.El, and a percent correct $<70\%$ for the remaining three parameters. The human fibula was misclassified as human femur in 54% of cases for On.Cr + On.Ar.

3.2.3 | Load-complexity category comparisons: What differences in osteon shape exist based on load-complexity category?

3.2.3.1 | ANOVA

When using an ANOVA design to analyze the different load-complexity categories in terms of the independent (nonmean) data, all categories (low, moderate, high) are significantly different for On.Cr ($p < .01$), but only between low- and high-complexity for On.El ($p = .02$). But, contrary to our expectations (Figure 2), the osteons with the most elliptical (hence least circular) shapes are not in the high-complexity category bone (sheep tibia, which has comparably more prevalent/predominant torsion/shear), but rather, are seen in the low-complexity load category (On.El = 1.39; On.Cr = 0.82) and the most circular osteons are seen in the moderate-complexity category (On.Cr = 0.87; Figure 5).

A subset analysis shows that this paradoxical finding is not due to the ellipticity of the osteons in the neutral axis regions of the low-complexity category bones because the percent differences between the neutral axis region vs. all other regions is $<2\%$ for On.Cr and for On.El. This is also true for all bones in each of the various load-

Discriminant Functional Analysis (DFA) for Species and Load-Complexity Category (On.Cr and On.Cr + On.Ar)

Species	Sorted by Circularity (On.Cr)					Sorted by Circularity + Area (On.Cr + On.Ar)			
	Chimpanzee	Deer	Horse	Human	Sheep	Deer	Horse	Human	Sheep
Chimpanzee	2 25%	1 12.5%	2 25%	0 0%	3 37.5%	—	—	—	—
Deer	2 40%	0 0%	3 60%	0 0%	0 0%	5 100%	0 0%	0 0%	0 0%
Horse	0 0%	3 20%	7 46.7%	1 6.7%	4 26.7%	0 0%	11 73.3%	0 0%	4 26.7%
Human	0 0%	0 0%	0 0%	37 100%	0 0%	0 0%	0 0%	37 100%	0 0%
Sheep	0 0%	0 0%	5 33.3%	0 0%	10 66.7%	4 27%	2 13.3%	0 0%	9 60%

Load-Complexity Category	Sorted by Circularity (On.Cr)			Sorted by Circularity + Area (On.Cr + On.Ar)		
	High	Moderate	Low	High	Moderate	Low
High	4 80%	0 0%	1 20%	5 100%	0 0%	0 0%
Moderate	3 5%	40 66.7%	17 28.3%	5 9.6%	36 69.2%	11 21.2%
Low	5 33.3%	0 0%	10 66.7%	7 46.7%	0 0%	8 53.3%

FIGURE 6 Results from DFA of the mean data for both differentiation of species (top) and load-complexity category (bottom) based on On.Cr, and On.Cr + On. Ar. The vertical column to the left represents the known species or load-complexity category. The actual classification based on either On.Cr or On.Cr + On.Ar is represented horizontally for each species or load-complexity category. For example, (1) deer bones were misclassified as equine bones in 60% of cases; (2) 80% of high-complexity loaded bones were correctly classified as high-complexity loading category. The top number represents the raw number of specimens for each classification; the percent below is the percent of the known specimen that was classified in a given category. On.Ar data were not available for the chimpanzee bones, and therefore not included in the DFA for On.Cr + On.Ar, demarcated by the solid line

complexity categories. However, the moderate-complexity category likely has the highest On.Cr due to the inclusion of the human specimens. This is further discussed below in the human versus nonhuman section (number 6). Additionally, although the most elliptically shaped osteons in all of the calcanei are in the sheep calcaneus where they are most elliptical in the neutral axis region, none of these differences are statistically significant within this simply loaded bone ("tension region": On.El = 1.49, On.Cr = 0.79; "neutral axis region": On.El = 1.52, On.Cr = 0.79; "compression region": On.El = 1.47, On.Cr = 0.79, for all $p > .5$). In fact, On.Cr in the sheep species is only statistically significantly different when sheep calcaneus (low-complexity category) is compared to the sheep tibia (high complexity) but not when compared to the sheep radius (moderate complexity; Figure 4).

The sheep tibia is the only high-complexity category bone in our analysis and had comparatively fewer osteons (total analyzed $n = 120$; ~ 17 /bone) than the other bones in our study. This reflects low fractional area of secondary osteonal bone (On.B.Ar/T.Ar; range from lateral cortex to cranial cortex: 0.3–26.0%). The low On.B.Ar/T.Ar in conjunction with the fact that sheep are docile in terms of their ambulatory activities (Skedros et al., 2011c), likely contributes to a smaller

interindividual variation in On.Cr seen in this otherwise "high-complexity" category bone, and might help to explain the presence of osteons that are more circular than expected. Additional discussion of these issues is considered below in the Discussion section.

3.2.3.2 | DFA

When using independent (nonmean) data to differentiate the three load-complexity categories (Figure 6) in terms of On.Cr + On.Ar, high complexity had a percent correct of 76%. For On.El + On.Ar, high complexity had a percent correct of 71%. For On.Cr + On.El + On.Ar, the high complexity had a percent correct of 78%. All remaining parameters for determining load-complexity category had a percent correct of <70%.

Using DFA of the quasi-nested data, the percent correct for classification of the high-complexity category was 100% for On.Cr + On.Ar + On.El and for On.Cr + On.Ar and was 80% for On.Ar + On.El, On.Cr, and On.Ar. All other factors for high complexity category and all factors for low and moderate complexity categories had a percent correct of <70%.

Although the regions of the human bones analyzed are in the moderate-complexity load category, they have the highest average On.

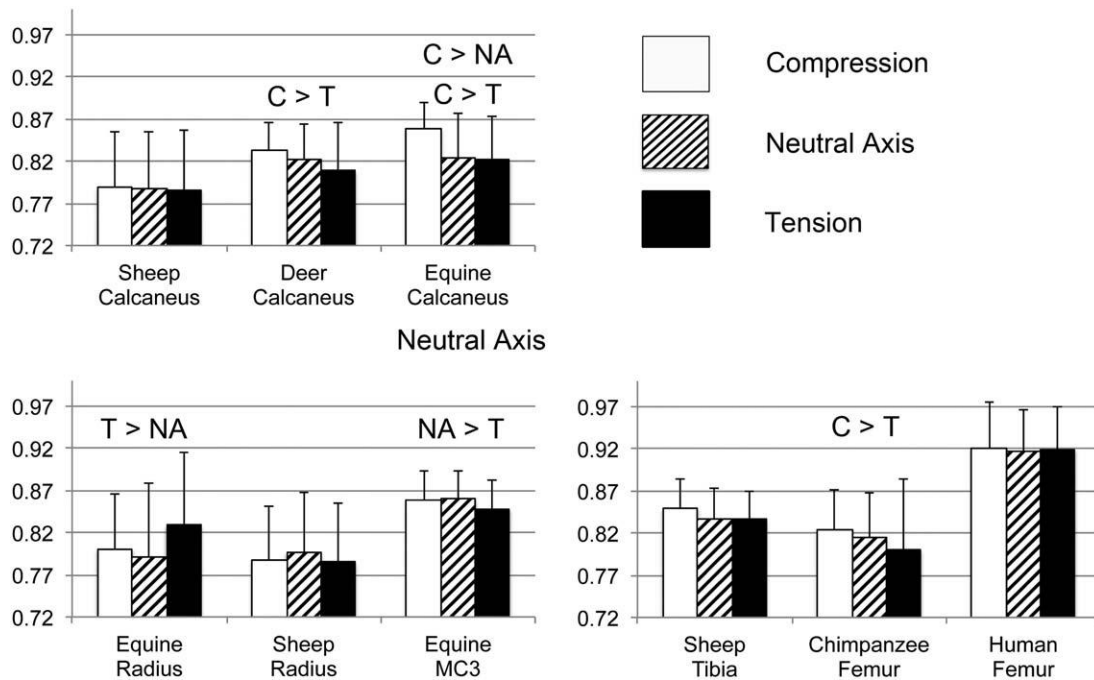


FIGURE 7 Bar graphs showing On.Cr (mean \pm SD) for tension (T), compression (C), and neutral axis (NA) regions for each species. (a) Nonprimate specimens that are in the low or moderate A complexity load categories; (b) nonprimate and primate specimens that are in the moderate B or high complexity load categories

Cr when compared with the other bones. Therefore, the human bones were differentiated from the other species with comparatively high accuracy (range: 84% for quasi-nested based on species to 100% for quasi-nested based on primates vs. nonprimates) using DFA of the On.Cr data. The high-complexity load category bones (i.e., sheep tibiae) have significantly lower average On.Cr values than the moderate-complexity category bones, and were classified correctly using DFA for On.Cr + On.Ar more often than the moderate- and low-complexity category bones (percent correct for quasi-nested) for independent (non-mean) data percent correct are: high 76%, moderate 61%, low 47%; for quasi-nested data percent correct are: high 100%, moderate 69%, low 53%. By contrast, when using independent (nonmean) for On.Cr data only, the high-complexity load category is classified correctly using DFA the least often when compared with moderate- and low-complexity categories.

The poor accuracy and contradictory nature of these DFA findings coupled with unexpectedly fewer elliptical osteons in the high-complexity category as shown in our ANOVA analysis, suggests that species determination based on On.Cr alone can be confounded by load history, especially among the nonhuman species (because of the greater number of bones having lower complexity loading).

3.2.4 | Strain-mode distributions: What differences in osteon shape exist based on habitual strain-mode?

3.2.4.1 | ANOVA

The ANOVA design was used to analyze differences in On.Cr and On.El for each species based on a habitual strain-mode (i.e., tension, compression, neutral axis) region (Figure 7). Significant differences were present in On.Cr of the chimpanzee femora and all of the equine bone

types, but only in two of the three equine bone types for On.El. For the equine calcanei, On.Cr was significantly greater (osteons are more circular) in “compression regions” compared with both “neutral axis regions” and “tension regions” ($p < .001$). For the equine radii On.Cr was also significantly greater in “compression regions” than “neutral axis regions” ($p = .001$), but with On.Cr trending to be greater in “tension regions” compared with “compression regions” ($p = .06$). For the equine MC3s On.Cr was not significantly greater in “compression regions” but was significantly greater in “neutral axis regions” compared to “tension regions” ($p = .03$). For the chimpanzee femora, On.Cr was significantly greater in “compression regions” compared with “tension regions” ($p = .04$). However, there were no statistically significant differences in On.Cr based on strain-mode distributions in the sheep calcanei, sheep radii, sheep tibiae, deer calcanei, human femora, or human fibulae. For the equine calcanei On.El was significantly greater in “neutral axis regions” compared with “compression regions” ($p < .001$) and in “tension regions” compared with “compression regions” ($p = .005$). For the equine radii, On.El was significantly greater in “neutral axis regions” compared with “tension regions” ($p < .001$) and trending greater in “compression regions” compared with “tension regions” ($p = .09$). However, there were no significant differences in On.El based on strain-mode distribution for the sheep calcanei, sheep radii, sheep tibiae, deer calcanei, equine third metacarpals, chimpanzee femora, human femora, or human fibulae.

3.2.4.2 | DFA

When using DFA of the independent data, with all species and bone types combined in the analysis to classify strain-mode distribution, “compression regions” were most often classified correctly compared

with “tension regions” and “neutral-axis regions” for all parameters with the exception of On.Cr (“tension region” classify correctly more often). However, the percent correct was <70% for all parameters and strain-modes. The range for percent correct was 21% (On.Cr) to 68% (On.Ar) for “compression regions,” 1% (On.Ar) to 48% (On.Cr) for “tension regions,” and 1% (On.El) to 21% (On.Ar + On.El) for “neutral-axis regions.” In several instances “tension-regions” were incorrectly classified as “compression regions” >50% of the time as follows: 50% for On.Cr + On.Ar, 51% for On.Ar + On.El, 58% for On.El, and 62% for On.Ar. “Neutral axis regions” were incorrectly classified as “compression regions” >50% of the time in two instances: 56% for On.El, and 62% for On.Ar.

When using DFA of the quasi-nested data, with all species and bone types combined in the analysis to classify strain-mode distribution, the percent correct for all strain-mode distributions was <70% for all parameters. When using On.Cr, “neutral-axis regions” were inappropriately classified as “tension regions” in 51% of cases. When using On.El, “tension regions” were inappropriately classified as “compression regions” in 51% of cases. When using On.Ar, “compression regions” were inappropriately classified as “tension regions” in 59% of cases and “neutral-axis regions” were inappropriately classified as “tension regions” in 54% of cases.

3.2.5 | Primates versus nonprimates: What differences in osteon shape exist for primate versus nonprimates?

3.2.5.1 | ANOVA

This analysis was aimed at detecting significant differences between the primates (chimpanzee femora, human femora, and human fibulae) and the nonprimates (deer calcanei, sheep calcanei, sheep radii, sheep tibiae, equine calcanei, equine radii, equine third metacarpals). Significant differences were found for On.Cr but not for On.El. On.Cr was significantly greater in primates (mean On.Cr: 0.89) compared with nonprimates (mean On.Cr: 0.82; $p < .001$).

3.2.5.2 | DFA

When using DFA for the independent (nonmean) data to differentiate primates from nonprimates, nonprimates had percent correct of 97% for On.Cr + On.El, 95% for On.Cr + On.Ar, 99% for On.Cr + On.El + On.Ar, 89% for On.El + On.Ar, and 89% for On.Ar. The percent correct for primates for On.Cr and for On.El were <70%. The percent correct for primates was 73% for On.Cr, 83% for On.Cr + On.El, 90% for On.Cr + On.Ar, and 96% for On.Cr + On.El + On.Ar. The percent correct for the remaining parameters was <70%. Additionally, nonprimates were misclassified as primates in 61% of cases for On.El.

When using DFA to classify between primate and nonprimate specimens, the percent correct for primate specimens was 84% for On.Cr, 82% for On.Cr + On.El, 100% for On.Cr + On.Ar, 100% for On.Cr + On.El + On.Ar, 84% for On.El + On.Ar, and 78% for On.Ar. The percent correct for nonprimates was 91% for On.Cr, 100% for On.Cr + On.El, On.Cr + On.Ar, On.Cr + On.El + On.Ar, and On.Ar, and 97% for On.El + On.Ar. The percent correct for both primate specimens and nonprimate specimens was <70% for On.El.

3.2.6 | Human versus nonhuman: What differences in osteon shape exist for humans versus nonhumans?

3.2.6.1 | ANOVA

When using ANOVAs to compare humans versus nonhumans, On.Cr was significantly greater in humans compared with nonhumans ($p < .001$). This was the case when comparing human versus nonhuman species collectively and when comparing human species vs. each of the nonhuman species independently (Figure 4a). By contrast there were no significant differences with respect to the On.El data.

3.2.6.2 | DFA

When using DFA of the independent (nonmean) data to distinguish human versus nonhuman specimens based on each parameter, nonhuman bones had a percent correct of 99% for On.Cr + On.El + On.Ar, 98% for On.Cr + On.El, 95% for On.Cr + On.Ar, 89% for On.El + On.Ar, 78% for On.Cr, and 89% for On.Ar. The percent correct for nonhuman bones was <70% for On.El. For human bones, the percent correct was 96% for On.Cr + On.El + On.Ar, 94% for On.Cr + On.El, 90% for On.Cr + On.Ar, and 86% for On.Cr. The percent correct for human bones was <70% for On.El + On.Ar, On.El, and On.Ar.

When using DFA of the quasi-nested data to distinguish between human vs. nonhuman specimens the percent correct was similarly high. For nonhuman bones, the percent correct was 98% for On.Cr, 100% for On.Cr + On.El, On.Cr + On.Ar, On.Cr + On.El + On.Ar, and On.Ar, and 97% for On.El + On.Ar. The percent correct for nonhuman bones for On.El was <70%. For human bones, the percent correct was 100% for On.Cr, On.Cr + On.El, On.Cr + On.Ar, and On.Cr + On.El + On.Ar, 84% for On.El + On.Ar, and 78% for On.Ar. As was the case for the nonhuman bones, the human bones also had a percent correct <70% for On.El.

A subset DFA of both the independent (nonmean) and quasi-nested data was done looking only at the chimpanzee femora and the human femora to determine if these species could be reliably distinguished based on On.Cr, On.El, and On.Cr + On.El. None of the remaining parameters used above were used in the subset analysis, as each includes On.Ar, which is not available for the chimpanzee femora. For the independent (nonmean) data, the percent correct for chimpanzee femora for On.Cr was 76%, and the percent correct for On.Cr + On.El was 92%. The percent correct for the human femora was 84% for On.Cr and 92% for On.Cr + On.El. For both chimpanzee femora and human femora, the percent correct for On.El was <70%. In fact, the chimpanzee femora were misclassified as human femora in 55% of cases for On.El. For the quasi-nested data, the percent correct for chimpanzee femora was 100% for On.Cr and On.Cr + On.El. The percent correct was <70% for chimpanzee femora for On.El. For the human femora, the percent correct was also 100% for On.Cr and On.Cr + On.El, and 71% for On.El. There were no misclassifications in this subset DFA for the quasi-nested data.

4 | DISCUSSION

The degree of correct classifications based on geometric osteon parameters in a DFA has been used in many studies as a method for

determining the taxonomic provenance of bones and bone fragments. However, the number of misclassifications has a tendency to be understated. While it could be argued that for the purposes of many studies in physical anthropology that these misclassifications are of little significance as long as the percent correctly classified is high for human versus nonhuman distinctions, this does not acknowledge the fact that many other factors are involved in prevalence and regional distributions of secondary osteons and in their specific morphological characteristics that are used to make these distinctions. For example, a reasonable explanation for the misclassification of sheep radii as equine radii in 60% of cases could be that the moderate-complexity loading shared by these specimens is what increases the probability that they will be indistinguishable. If the question is whether or not the bone fragment came from a human, then the importance of this distinction might seem to be of lesser significance in addition to the possibility that it might be confounded by the likelihood that mid-diaphyses of many human limb bones are in the high-complexity load category. However, misidentification of human specimens as nonhuman specimens becomes more likely when considering the possibility that load-complexity category and prevalent/predominant habitual strain-mode distribution can have strong influences in determining osteon shape in some locations of human limb bones (e.g., mid-diaphyses of the tibia and fibula, and proximal diaphysis of the femur; **Figure 1**). In this study, strain-mode distribution was misclassified in >50% of cases in the DFA of independent and quasi-nested data.

Our results strongly suggest that species, strain-mode distribution, and load-complexity category do not strongly account for the variation that exists in osteon shape. While On.Cr is considered a new metric for determining if an unknown bone fragment is of human origin, it has little utility in other inter-species comparisons, or in understanding histological bone adaptation to a habitual load environment.

In addition to habitual load-complexity and habitual strain-mode distributions, effects associated with aging, sex, and body weight (discussed below), and genetic variations and developmental constraints that could influence the emergence of specific histomorphological characteristics and/or their regional distribution might help to explain the frequent misclassifications among the nonhuman comparisons (Bromage and Boyde, 1998; de Margerie et al., 2002; Havill, 2003; Havill et al., 2013; Lee, 2004; Skedros and Hunt, 2004; Starck and Chinsamy, 2002; Warshaw, 2007). For example, a study of middle-aged human female twins found between 55 and 62% of remodeling marker differences are attributable to genetic factors (Bjørnerem et al., 2015; remodeling markers included: serum osteocalcin, C-terminal cross-linking telopeptide of type I collagen, and procollagen type I N-terminal propeptide). In their histomorphometric analysis of 101 baboon femora (ages 7–33 years) sectioned transversely at mid-diaphysis, Havill et al. (2013) found significant genetic effects for On.Ar, On.B.Ar/T.Ar, and wall thickness of secondary osteons (On.Cr and On.El were not analyzed). This corresponds to 48–75% of the total phenotypic variance of these three cortical microstructural characteristics. By contrast, they found no evidence that On.N/T.Ar and porosity were heritable. Hence, the parameter most susceptible and reflective

of genetic effects is osteon size. In the perspective of these findings (and if they can be broadly extrapolated to other mammalian species), it seems reasonable to conclude that On.Cr is not heritable because we found little or no correlation of this characteristic with On.Ar in the primate and nonprimate bones. Regardless of the specific reasons for the frequent misclassifications in the nonhuman comparisons, it is clear that an important role is played by the statistically significant regional differences in these osteon shape characteristics examined herein, as shown in many cases between the bone “types” within the sheep (calcanei, radii, tibiae) and horses (calcanei, radii, MC3s; **Figure 4**). Consequently, a fragment of a sheep tibia (mean On.Cr = 0.84) could be inadvertently misclassified as being from a horse (range of mean On.Cr values = 0.80–0.86). This result is indicative of the weakness of using On.Cr for nonhuman species differentiation. While distinguishing between two nonhuman species may not be of direct benefit to biological anthropologists, the inconsistency in being able to do so supports the need for caution when using On.Cr in interpreting load history.

When mean and nonmean On.Cr and On.El data were examined independently and in analyses that coupled these characteristics (and with On.Ar), they also proved to be generally poor in terms of distinguishing among (1) the different load-complexity categories of all bones studied, and (2) the regional variations in strain-mode distributions in the bones experiencing habitual bending (which included all bones except for the sheep tibia). In fact, these osteon shape characteristics have little value in terms of predicting load history, even in relatively simply loaded calcanei (none of the calcanei from the three species studied showed all of the expected regional variations). By contrast, a series of prior investigations using the same bones examined herein demonstrate that between- or within-bone patterns of predominant CFO and osteon collagen/lamellar “morphotypes” are much stronger correlates in these contexts, and even more strongly than On.N/T.Ar and On.Ar (Skedros, 2012; Skedros and Keenan 2016; Skedros et al., 2004, 2009, 2011a, 2011b, 2013a). Therefore, the results of this investigation sustain the preeminent status that these CFO-based characteristics have, when compared with all other histomorphological and compositional parameters studied, in terms of (1) identifying the strain-mode distributions in bones that have the capacity for osteonal renewal and are habitually loaded in bending (i.e., in the low- and moderate-complexity load categories), and (2) distinguishing torsional versus bending load histories (Skedros, 2012; Skedros et al., 2009). To our knowledge, the ability of variations in predominant CFO across a bone's cross-section to differentiate species has not been studied.

The result achieved in this study in differentiating human from nonhuman bones should be considered with caution due to of the variability in On.Cr data reported previously for human specimens. Some studies report humans as having an On.Cr that is on average lower than nonhuman species (Crescimanno and Stout, 2012; Tersigni et al., 2008; Tersigni-Tarrant et al., 2011); this study and other prior studies have reported greater human mean On.Cr values (Dominguez and Crowder, 2012; Skedros et al., 2014a). Perhaps, as alluded to by Crescimanno and Stout (2012), when compared to the nonhuman species studied in this context there is relatively greater interindividual

variability in osteon shape in human bones that results in a broader range of On.Cr. We have also considered interspecies and intraindividual differences in habitual ambulatory activities in the bones/species examined in the present study (Skedros et al., 2006, 2007a, 2011c). In addition to the effect of advanced aging on osteoclast activity (which is most important in determining osteon size and shape) (Qiu et al., 2010), the discrepancies in human On.Cr data might also be influenced by a lack of standardized methods for obtaining On.Cr (Mears et al., 2014, 2015). It would be advisable to employ caution when using On.Cr to differentiate humans from other species while the reason for this discrepancy remains unclear.

The studies by Crescimanno and Stout (2012) nor Dominguez and Crowder (2012) did not provide data that quantitatively considered the possibility that the bones that they examined might have regional variations in osteon morphology that can be adaptations for their load histories; this study adds this analysis. In addition to evaluating osteons from strictly defined anatomical quadrants, these investigators also eliminated some osteons (percent eliminated not reported) based on noncircular Haversian canal shapes. By contrast, we could not determine the impact that eliminating vs. not eliminating osteons would have on our results because we did not quantify the shapes of the Haversian canals. Crescimanno and Stout (2012) excluded osteons with Haversian canals having a circularity index <0.9 ($1.0 =$ perfect circle); Dominguez and Crowder (2012) excluded osteons with Haversian canals that have “excessively” elliptical shapes (i.e., maximum:minimum Haversian canal diameter ratios $\geq 2:1$; **Figure 3c**). These exclusion criteria reflect the assumptions that an osteon with an excessively noncircular Haversian canal is likely the result of its oblique orientation in three dimensions (3D), which warrants elimination because the cross-sectional area of the osteon would otherwise not be adequately quantified (personal communications: C. Crowder and S. Stout). What follows is an example showing why eliminating osteons that do course obliquely in 3D could be problematic in some cases when using On.Cr and/or On.El to distinguish species—especially when the cross-sections being analyzed have regionally heterogeneous On.Cr and/or On.El that are important adaptations because they accommodate differing mechanical demands.

The elliptical shape of an osteon in two dimensions (2D) can reflect its oblique orientation in 3D, which is logical if the osteon resembles a simple cylinder (Hennig et al., 2015; Mohsin et al., 2006; Parfitt, 1994). It has been suggested that this 3D obliquity with respect to the long axis of the bone diaphysis, hence increased On.El (and decreased On.Cr) when viewed in a 2D transverse section, can be mechanically adaptive in some bones where this is thought to enhance tissue mechanical toughness (Skedros et al., 2013a, 2014a). This could be an adaptation for the relatively diffusely distributed shear strains and obliquely oriented principal strains in bones that experience habitual torsion (e.g., sheep tibia, mid-shaft human femur, or other high-complexity loaded bones or regions) or for these and other strain characteristics that are more localized in the vicinity of the neutral axis regions in bones subjected to relatively simple bending (Lanyon and Bourn, 1979; Martin and Burr, 1989; Petrýl et al., 1996; Skedros,

2012; Skedros et al., 2007b,a; Sorenson et al., 2004; Su et al., 1999). By contrast, some bones with regions habitually loaded in prevalent/predominant tension are known to have osteons with various noncircular shapes that are not typically elliptical (Skedros et al., 2001, 2007b). This is a case where On.Cr does not reveal all “types” of noncircular osteons that can be mechanically adaptive. An example of this has been reported in the deer calcaneus [a simple bending model (Sinclair et al., 2013)] where the relatively increased On.El occurs in the medial and lateral cortices (i.e., “neutral axis regions”) but not in the plantar “tension” cortex, although these two regions have low On.Cr (i.e., relatively “noncircular” osteons; **Figure 3**; Skedros et al., 2007a, 2014a; Sorenson et al., 2004). The different microstructural adaptations in these different locations likely reflect differential/regional mechanical benefits of (1) increased interfacial complexity provided by highly noncircular (but not strongly elliptical) osteons in the plantar “tension” cortex (Bigley et al., 2006; Hiller et al., 2003), and/or (2) the reduction in deleterious effects of shear stresses provided by 3D osteon obliquity (strongly elliptically shaped) in the medial-lateral “neutral axis/predominant shear” region (Ascenzi and Bonucci, 1968, 1972; Martin and Burr, 1989). Hence, in the neutral axis region of the deer calcaneus, 3D osteon obliquity is most likely the proximate biomechanical reason for the 2D osteon elliptical shapes, but 3D osteon obliquity does not likely explain the irregular (but not strongly elliptical) shapes in the plantar “tension” cortex.

This example in the deer calcaneus demonstrates that the evaluation of both On.Cr and On.El is necessary for a complete analysis of osteon shape variations when comparing bones of varying load complexity, especially in bones from the low- and moderate-complexity load categories (because they typically have a consistent neutral axis region during typical loading conditions). It has also been shown that when criteria based on the shape of an osteon’s Haversian canal (Crescimanno and Stout, 2012; Dominguez and Crowder, 2012) are used to eliminate the quantification of some osteons in the deer calcaneus model that (1) this can remove nearly 70% of the osteons when using the circularity elimination criterion of <0.9 and 45% of the osteons when using the On.El elimination criterion of $\geq 2:1$, and (2) the statistical analysis conducted after the elimination of these osteons results in an inaccurate interpretation of the load history of this simply loaded bone (Skedros et al., 2014b; **Figure 3**). Additional studies are needed that critically examine the methods and rationales for using osteon selection/exclusion criteria to more rigorously determine if (1) they are in fact necessary in studies aimed at differentiating species (if they are, then Haversian canal shape and osteon shape must always be determined for each osteon), and (2) how they might affect the results of studies that focus on species differentiation versus the results of studies that mainly consider higher-complexity category bones where, when compared with the lower-complexity bones, the elimination criteria might seem less important in affecting the results. This is because high-complexity loaded bones, by lacking a consistent neutral axis region, do not have the marked regional strain-mode-specific histomorphological adaptations seen in low-complexity loaded bones (Skedros, 2012; Skedros et al., 2006). It is important to emphasize this distinction because anthropological studies of bone histomorphological adaptation

often use bones in the high-complexity load category (Hillier and Bell, 2007; McFarlin et al., 2016; Skedros et al., 2015; Warshaw, 2008).

The osteons from the sheep tibiae did not exhibit the relatively greater elliptical shapes that we expected for a bone in the high-complexity load category. What initially led us to expect that osteons would generally be more elliptical in this bone were the findings of Lanyon and Bourn (1979) in tibiae of domesticated sheep, and Heřt et al. (1994) and Petrtýl et al. (1996) in various limb bones of modern humans. The latter two studies examined epifluorescent images of India ink-stained coronally sectioned preparations of mid-diaphyseal regions (after ~2 mm of the bone was sanded off of the bone surface and the sanded surface was polished) of femora, tibiae, humeri, radii, and ulnae. In their 2D analysis of the human femora at mid-diaphysis, which is characterized as a high-complexity category region because it is subject to high torsion with bending (Skedros 2012), they concluded that the secondary osteons are typically aligned close to the directions of the principal stresses, which were calculated using an analytical model based on cadaver bones. They found that the osteons at the femoral mid-diaphysis deviate 6–10° with respect to the long axis of the bone, which closely corresponds to the orientation of the calculated principal stresses. In the other bone “types” the osteons were also found to run obliquely with respect to the longitudinal axis of the bones: (1) tibiae 6–8°, (2) humeri 12–15°, (3) radii ~8°, and (4) ulnae ~8°. Based on *in vivo* strain data from sheep tibiae, Lanyon and Bourn (1979) reported principal strains on the order of 28.8° in the cranial cortex and 22.4° in the caudal cortex. In view of these sheep and human data, we predicted that our “moderate” and “high-complexity” load category bones would have secondary osteons that also course obliquely, on the order of 10°–30° from the long axis of the diaphysis. Hence, assuming that a typical osteon resembles a simple cylinder, we predicted that 3D obliquity would produce these 2D variations (1) for 10° tilt, On.Cr of 0.84 and On.El of 1.02, (2) for 20° tilt, On.Cr of 0.83 and On.El of 1.07, and (3) for 30° tilt, On.Cr of 0.82 and On.El of 1.16 (these values were calculated in ImageJ using simulated osteons with Howship’s lacunae, and with all osteons having the same On.Ar; Mears et al., 2015). However, we did not find significantly increased On.El in the sheep tibia or in the bones with localized high shear (neutral axis) regions. This might reflect (1) osteon 3D obliquity that is much less than expected in high-complexity loaded bones and does not differ much (contrary to our expectations) across the range of load complexity, and/or (2) the shape of an osteon can change independent of its 3D orientation as has been suggested by Hennig et al. (2015) and shown in Figure 5 of Skedros et al. (2007b).

Support for the former possibility includes the only study that we are aware of that determined the relationship of secondary osteons with principal strains based on *in vivo* strain measurements. In that study, Lanyon and Bourn (1979) used polarized light to examine 100 μm thick coronal sections of mature sheep tibiae and showed that, in contrast to the conclusions of Heřt, Petrtýl, and coworkers’ in mid diaphyses of human limb bones, osteon orientation was not closely aligned with the principal strain direction: (1) in the cranial cortex the osteons are oriented 11.5° with respect to the long axis of the sheep

tibia whereas the principal strain direction is 28.8°, and (2) in the caudal cortex the osteons are oriented 9.5° with respect to the long axis of the sheep tibia whereas the principal strain direction is 22.4°. Perhaps osteon 3D deviations on the order of 10° from the long axis are not sufficient to produce the magnitude of elliptically shaped osteons that we expected in this high-complexity loaded bone. To more rigorously investigate details of the relationship between 3D osteon orientations and their 2D cross-sectional shapes, 3D reconstructions from serial sections (Cohen and Harris, 1958; Maggiano et al., 2016) will be needed because the current capacity of high-resolution 3D computed tomography is not sufficiently accurate (Hennig et al., 2015).

Although On.Cr is greatest (and On.El is paradoxically lowest) in the sheep tibia when compared to sheep radii and calcanei, we only measured ~17 osteons in each sheep tibia. Therefore, the comparisons we made with the sheep tibiae must be viewed with caution because of the possibility of reduced statistical power in addition to the possibility that these osteons might reflect very localized adaptation for the shear/tension strain milieu of the cranial cortex (>90% of the sheep tibia osteons that we quantified were found in this region) (Lanyon and Bourn, 1979; Skedros et al., 2009). However, the seemingly small number of osteons quantified in our seven sheep tibiae is not an unusual sample size in studies dealing with species differentiation. For example, Martiniaková et al. (2006) obtained ~25 osteons/bone in the species that they examined, and they and Harsányi (1993) recommend obtaining data from 50 to 100 osteons per species. Crescimanno and Stout (2012) examined 12 osteons per bone (which they then averaged to obtain one value for each bone). In contrast, Dominguez and Crowder (2012) tried to examine at least 50 osteons/rib and 50 osteons/quadrant in the each of the four quadrants that they examined in each of their limb bones. The fewest number of osteons analyzed was 31/bone, which was from a fragmented deer rib. These examples expose an important but unanswered question that has even broader implications: what percent of secondary osteonal bone (On.B.Ar/T.Ar) is needed for differences in histomorphological characteristics of secondary osteons to be considered relevant for distinguishing species or for interpreting the load history of a bone or bone region? In other words, what percentage of a cortical area must be remodeled with secondary osteons to consider functional adaptation in terms of the secondary osteonal bone rather than primary bone? For example, it seems likely that the On.B.Ar/T.Ar of the sheep tibia is so low that mean osteon circularity values are not relevant for distinguishing this bone from the others when using load history criteria. Although there are a few studies that have obtained data where this issue can be indirectly addressed in the context of bone mechanical properties (Carter et al., 1976; Currey, 2002; Kim et al., 2007; Mayya et al., 2013; Riggs et al., 1993a, 1993b), we could not locate any studies that have specifically addressed this question in terms of the various contexts considered in the present study. Additional studies are needed to determine if there is a “threshold” On.B.Ar/T.Ar where histological differences resulting from variations in secondary osteonal characteristics can be considered important in terms of the functional adaptation of a bone or bone region.

Several of the studies compiled in the review of Hillier and Bell (2007) have shown that differences in histological type (fibrolamellar

vs. secondary osteonal) are most successful in differentiating human bones from dog and deer bones. Additionally, human bones can also be readily distinguished from dog and deer bones based on differences in Haversian canal diameter, osteon diameter, and On.N/T.Ar. The species that follow dog and deer bones in terms of the success rate in being distinguished from various nonhuman bones based on relatively simple osteonal characteristics include bones from domesticated cats (*Felis silvestris catus*), Snowshoe and European hares, European badgers, and raccoon dogs (*Nyctereutes prodyonoides*). By contrast, cow, goat, sheep, pig, horse, and water buffalo bones have been shown to be successfully differentiated by the presence versus absence of fibrolamellar bone and not by these osteonal characteristics. Although there are studies that have led to the conclusion that it is generally safe to assume that a bone fragment that is primarily fibrolamellar is nonhuman, it is not correct to conclude that a fragment that is primarily comprised of secondary osteons is likely human. For example, in adult cows, sheep, horses, deer, and various nonhuman primates, it is well known that there can be regions of a diaphyseal cross-sections of limb bones that are highly remodeled with secondary osteons while other regions of the same cross-sections are primarily, or solely, fibrolamellar (Carter et al., 1976; Mason et al., 1995; Schaffler and Burr, 1984; Skedros et al., 2003b; Stover et al., 1992). Faulty interpretations of load history can also result when differences in the prevalence and distribution of secondary osteons and/or predominant CFO are used to distinguish between bones in the high-complexity load category (where these variations are not helpful) vs. the moderate- and low-complexity load categories (where these variations are helpful; Skedros, 2012). This is especially true when regional strain-mode-related histomorphological adaptations are anticipated but the concept of load-complexity and/or the "priority" of shear-strain-related adaptations is not recognized (e.g., Goldman et al., 2003; Lee, 2004; Mayya et al., 2013; Skedros et al., 2015; Zedda et al., 2015).

Although we have found the load-complexity categories to be very useful because they help provide clarity in many studies of limb-bone adaptation (Skedros, 2012, 2014; Skedros et al., 2006, 2009, 2011c, 2013a), important limitations include the paucity of in vivo strain data in anthropoid bones and the imperfect criteria used to designate the categories—defined by the magnitude of change in neutral axis location during habitual/controlled ambulation. We recognize that less frequent natural gait-related activities can shift the neutral axis beyond the "habitual range" and this, even if very brief, might be sufficient to evoke cortical bone adaptation that confounds attempts to make simple interpretations (Main, 2007; Moreno et al., 2008; Rubin et al., 2013). Our designation of "neutral axis regions" is also least rigorous in bones in the moderate-complexity categories (i.e., there is a greater potential for overlap in these bones with the other categories; Skedros et al., 2006), which is the main reason why we conducted our statistical analyses using data from the moderate A and B categories combined into one category. Rubin et al. (2013), Skedros et al. (2006), and Judex et al. (1997) discuss various problems with the assumption that characteristics of peak stresses or strains are important in causing regional variations in bone histomorphological adaptation.

Additional important limitations of the present study are that we could not assess include the potential effect of aging, sex, and body size in our samples (Britz et al., 2009; Cooper et al., 2007; Feik et al., 1996; Havill et al., 2013). The oldest human that we analyzed was only 71 years old and all the nonhuman bones were purposely selected from healthy younger adult animals. Also, body size data were typically unavailable and the sample sizes were too small to discern potential sex-related influences. Larger samples of bones spanning broad age ranges from individuals of known sex and body weight are needed to adequately determine if these factors influence osteon geometric characteristics, as has been shown in terms of increased On.Cr with advanced age in modern human femora (Britz et al., 2009; Currey, 1964).

5 | CONCLUSION

Results of this study support the conclusion that mean and nonmean (i.e., data from all osteons) On.Cr and On.El data, when considered independently or in terms of each of these characteristics coupled with each other and/or with On.Ar in a DFA, have limited value when used to distinguish load-complexity categories, regional prevalent/predominant strain-mode distributions in bone regions habitually loaded in bending, and among nonhuman species. In contrast, when distinguishing human from nonhuman bones the independent analysis of On.Cr was highly accurate (exceeding 95%) and was similarly accurate when considering On.Cr + On.Ar in a DFA. Other histomorphological characteristics of cortical bone that have been shown to be more reliable for distinguishing among load-complexity categories and other details of the load histories of various types of limb bones include regional, and often strain-mode-related, patterns of predominant CFO and secondary osteon collagen/lamellar morphotypes. However, these characteristics have not been evaluated in the context of species differentiation.

ACKNOWLEDGEMENTS

We thank Greg Stoddard for his assistance in statistical analysis. We also thank Dr. Roy Bloebaum for laboratory support.

NOTES

¹ In this study all mentions of "osteons" refer to secondary osteons (Haversian systems). Primary osteons are not considered in this study. On.N/T.Ar represents the number of secondary osteons per total area of bone in the analysis region (T.Ar also includes osteon porosity, such as osteocytic lacunae and central canals; Skedros et al., 2013a).

² The three strain modes are: tension, compression, and shear.

REFERENCES

- Ascenzi, A., & Bonucci, E. (1968). The compressive properties of single osteons. *Anatomical Record*, *161*, 377–391.
- Ascenzi, A., & Bonucci, E., (1972). The shearing properties of single osteons. *Anatomical Record*, *172*, 499–510.
- Beckstrom, A. B. (2010). Histologic and geometric data challenge the assumption of habitual superior-inferior (tension-compression)

- bending across the chimpanzee proximal femur (pp. 1-319). Salt Lake City: University of Utah (Thesis).
- Beraudi, A., Stea, S., Bordini, B., Baleani, M., & Viceconti, M., (2010). Osteon classification in human fibular shaft by circularly polarized light. *Cells Tissues Organs*, 191, 260-268.
- Biewener, A. A., & Bertram, J. E. A. (1993). Mechanical loading and bone growth *in vivo*. In: Hall BK (Ed.), *Bone* (Vol. 7, pp. 1-36), Bone Growth - B. Boca Raton, Florida, USA: CRC Press.
- Biewener, A. A., & Dial, K. P. (1995). In vivo strain in the humerus of pigeons (*Columba livia*) during flight. *Journal of Morphology*, 225, 61-75.
- Biewener, A. A., Fazzalari, N. L., Konieczynski, D. D., & Baudinette, R. V. (1996). Adaptive changes in trabecular architecture in relation to functional strain patterns and disuse. *Bone*, 19, 1-8.
- Biewener, A. A., Swartz, S. M., & Bertram, J. E. A. (1986). Bone modeling during growth: Dynamic strain equilibrium in the chick tibiotarsus. *Calcified Tissue International*, 39, 390-395.
- Bigley, R. F., Griffin, L. V., Christensen, L., & Vandenbosch, R. (2006). Osteonal interfacial strength and histomorphometry of equine cortical bone. *Journal of Biomechanics*, 39, 1629-1640.
- Bjørnerem, A., Bui, M., Wang, X., Ghasem-Zadeh, A., Hopper, J. L., Zebaze, R., & Seeman, E. (2015). Genetic and environmental variances of bone microarchitecture and bone remodeling markers: A twin study. *Journal of Bone and Mineral Research*, 30, 519-527.
- Blob, R. W., & Biewener, A. A. (1999). In vivo locomotor strain in the hindlimb bones of Alligator mississippiensis and Iguana iguana: Implications for the evolution of limb bone safety factor and non-sprawling limb posture. *Journal of Experimental Biology*, 202, 1023-1046.
- Brits, D., Steyn, M., & L'Abbe, E. N. (2014). A histomorphological analysis of human and non-human femora. *International Journal of Legal Medicine*, 128, 369-377.
- Britz, H. M., Thomas, C. D., Clement, J. G., & Cooper, D. M. (2009). The relation of femoral osteon geometry to age, sex, height and weight. *Bone*, 45, 77-83.
- Bromage, T. G., & Boyde, A. (1998). Intracortical remodeling and growth of the macaque mandible. *Scanning*, 20, 240.
- Burr, D. B., Milgrom, C., Fyhrie, D., Forwood, M., Nyska, M., Finestone, A., . . . Simkin, A. (1996). In vivo measurement of human tibial strains during vigorous activity. *Bone*, 18, 405-410.
- Burr, D. B., Ruff, C. B., & Thompson, D. D. (1990). Patterns of skeletal histologic change through time: comparison of an archaic native American population with modern populations. *Anatomical Record*, 226, 307-313.
- Carrano, M. T., & Biewener, A. A. (1999). Experimental alteration of limb posture in the chicken (*Gallus gallus*) and its bearing on the use of birds as analogs for dinosaur locomotion. *Journal of Morphology*, 240, 237-249.
- Carando, S., Portigliatti Barbos, M., Ascenzi, A., & Boyde, A. (1989). Orientation of collagen in human tibial and fibula shaft and possible correlation with mechanical properties. *Bone*, 10, 139-142.
- Carter, D. R., Hayes, W. C., & Schurman, D. J. (1976). Fatigue life of compact bone-II. Effects of microstructure and density. *Journal of Biomechanics*, 9, 211-218.
- Carter, D. R., Smith, D. J., Spengler, D. M., Daly, C. H., & Frankel, V. H. (1980). Measurements and analysis of in vivo bone strains on the canine radius and ulna. *Journal of Biomechanics*, 13, 27-38.
- Cattaneo, C., DiMartino, S., Scali, S., Craig, O. E., Grandi, M., & Sokol, R. J. (1999). Determining the human origin of fragments of burnt bone: A comparative study of histological, immunological and DNA techniques. *Forensic Science International*, 102, 181-191.
- Cattaneo, C., Porta, D., Gibelli, D., & Gamba, C. (2009). Histological determination of the human origin of bone fragments. *Journal - Forensic Science Society*, 54, 531-533.
- Cohen, J., & Harris, W. H. (1958). The three-dimensional anatomy of haversian systems. *Journal of Bone and Joint Surgery. American Volume*, 40, 419-434.
- Coleman, J. C., Hart, R. T., Owan, I., Takano, Y., & Burr, D. B. (2002). Characterization of dynamic three-dimensional strain fields in the canine radius. *Journal of Biomechanics*, 35, 1677-1683.
- Cooper, D. M., Thomas, C. D., Clement, J. G., Turinsky, A. L., Sensen, C. W., & Hallgrímsson, B. (2007). Age-dependent change in the 3D structure of cortical porosity at the human femoral midshaft. *Bone*, 40, 957-965.
- Crescimanno, A., & Stout, S. D. (2012). Differentiating fragmented human and nonhuman long bone using osteon circularity. *Journal - Forensic Science Society*, 57, 287-294.
- Cristofolini, L., Viceconti, M., Cappello, A., & Toni, A. (1996). Mechanical validation of whole bone composite femur models. *Journal of Biomechanics*, 29, 525-535.
- Currey, J. D. (1964). Some effects of aging in human Haversian systems. *Journal of Anatomy London*, 98, 69-75.
- Currey, J. D. (2002). *Bones: Structure and mechanics* (pp. 436). Princeton, New Jersey, USA: Princeton University Press.
- de Margerie, E., Cubo, J., & Castanet, J. (2002). Bone typology and growth rate: Testing and quantifying 'Amprino's rule' in the mallard (*Anas platyrhynchos*). *Comptes Rendus Biologies*, 325, 221-230.
- Demes, B. (2007). In vivo bone strain and bone functional adaptation. *American Journal of Physical Anthropology*, 133, 717-722.
- Demes, B., Qin, Y. X., Stern, J. T., Jr., Larson, S. G., & Rubin, C. T. (2001). Patterns of strain in the macaque tibia during functional activity. *American Journal of Physical Anthropology*, 116, 257-265.
- Demes, B., Stern, J. T. Jr., Hausman, M. R., Larson, S. G., McLeod, K. J., & Rubin, C. T. (1998). Patterns of strain in the macaque ulna during functional activity. *American Journal of Physical Anthropology*, 106, 87-100.
- Dominguez, V. M., & Agnew, A. M. (2016). Examination of factors potentially influencing osteon size in the human rib. *Anatomical Record (Hoboken)*, 299, 313-324.
- Dominguez, V. M., & Crowder, C. M. (2012). The utility of osteon shape and circularity for differentiating human and nonhuman Haversian bone. *American Journal of Physical Anthropology*, 54, 84-91.
- Drapeau, M. S., & Streeter, M. A. (2006). Modeling and remodeling responses to normal loading in the human lower limb. *American Journal of Physical Anthropology*, 129, 403-409.
- Evans, F. G., & Riola, M. L. (1970). Relations between the fatigue life and histology of adult human cortical bone. *Journal of Bone and Joint Surgery. American Volume*, 52, 1579-1587.
- Feik, S. A., Thomas, C. D., & Clement, J. G. (1996). Age trends in remodeling of the femoral midshaft differ between the sexes. *Journal of Orthopaedic Research*, 14, 590-597.
- Gibson, V. A., Stover, S. M., Gibeling, J. C., Hazelwood, S. J., & Martin, R. B. (2006). Osteonal effects on elastic modulus and fatigue life in equine bone. *Journal of Biomechanics*, 39, 217-225.
- Goldman, H. M., Bromage, T. G., Thomas, C. D., & Clement, J. G. (2003). Preferred collagen fiber orientation in the human mid-shaft femur. *Anatomical Record*, 272A, 434-445.
- Goliath, J. R., Stewart, M. C., & Stout, S. D. (2016). Variation in osteon histomorphometrics and their impact on age-at-death estimation in older individuals. *Forensic Science International*, 262, 282.e281-282.e286.

- Gross, T. S., McLeod, K. J., & Rubin, C. T. (1992). Characterizing bone strain distribution in vivo using three triple rosette strain gauges. *Journal of Biomechanics*, 25, 1081–1087.
- Harsányi, L. (1993). Differential diagnosis of human and animal bone. In: G. Grupe and A.N. Garland, editors, *Histology of Ancient Human Bone: Methods and Diagnosis*, pp. 79–94, Proceedings of the "Palaeohistology Workshop" held in Göttingen Oct. 1990. Springer-Verlag, Berlin.
- Havill, L. M. (2003). Osteon remodeling dynamics in the Cayo Santiago *Macaca mulatta*: The effect of matriline. *American Journal of Physical Anthropology*, 121, 354–360.
- Havill, L. M. (2004). Osteon remodeling dynamics in *Macaca mulatta*: normal variation with regard to age, sex, and skeletal maturity. *Calcified Tissue International*, 74, 95–102.
- Havill, L. M., Allen, M. R., Harris, J. A., Levine, S. M., Coan, H. B., Mahaney, M. C., & Nicolella, D. P. (2013). Intracortical bone remodeling variation shows strong genetic effects. *Calcified Tissue International*, 93, 472–480.
- Hennig, C., Thomas, C. D., Clement, J. G., & Cooper, D. M. (2015). Does 3D orientation account for variation in osteon morphology assessed by 2D histology? *Journal of Anatomy*, 227, 497–505.
- Hillier, M., & Bell, L. (2007). Differentiating human bone from animal bone: a review of histological methods. *Journal - Forensic Science Society*, 52, 249–263.
- Hiller, L. P., Stover, S. M., Gibson, V. A., Gibeling, J. C., Prater, C. S., Hazelwood, S. J., ... Martin, R. B. (2003). Osteon pullout in the equine third metacarpal bone: effects of ex vivo fatigue. *Journal of Orthopaedic Research*, 21, 481–488.
- Iwaniec, U. T., Crenshaw, T. D., Schoeninger, M. J., Stout, S. D., & Erickson, M. F. (1998). Methods for improving the efficiency of estimating total osteon density in the human anterior mid-diaphyseal femur. *American Journal of Physical Anthropology*, 107, 13–24.
- Judex, S., Gross, T. S., & Zernicke, R. F. (1997). Strain gradients correlate with sites of exercise-induced bone-forming surfaces in adult skeleton. *Journal of Bone and Mineral Research*, 12, 1737–1745.
- Kalmey, J. K., & Lovejoy, C. O. (2002). Collagen fiber orientation in the femoral necks of apes and humans: Do their histological structures reflect differences in locomotor loading? *Bone*, 31, 327–332.
- Kim, J. H., Niinomi, M., Akahori, T., & Toda, H. (2007). Fatigue properties of bovine compact bones that have different microstructures. *International Journal of Fatigue*, 29, 1039–1050.
- Lambert, K. L. (1971). The weight-bearing function of the fibula. A strain gauge study. *Journal of Bone and Joint Surgery. American Volume*, 53, 507–513.
- Lanyon, L. E. (1974). Experimental support for the trajectorial theory of bone structure. *Journal of Bone and Joint Surgery. British Volume*, 56, 160–166.
- Lanyon, L. E., & Bourn, S. (1979). The influence of mechanical function on the development and remodeling of the tibia: an experimental study in sheep. *Journal of Bone and Joint Surgery. American Volume*, 61, 263–273.
- Lanyon, L. E., Goodship, A. E., Pye, C. J., & MacFie, J. H. (1982). Mechanically adaptive bone remodeling. *Journal of Biomechanics*, 15, 141–154.
- Lanyon, L. E., Hampson, W. G., Goodship, A. E., & Shah, J. S. (1975). Bone deformation recorded in vivo from strain gauges attached to the human tibial shaft. *Acta Orthopaedica Scandinavica*, 46, 256–268.
- Launey, M. E., Buehler, M. J., & Ritchie, R. O. (2010). On the mechanistic origins of toughness in bone. *Annual Review of Materials Research*, 40, 25–53.
- Lee, A. H. (2004). Histological organization and its relationship to function in the femur of Alligator mississippiensis. *Journal of Anatomy*, 204, 197–207.
- Lieberman, D. E., Pearson, O. M., Polk, J. D., Demes, B., & Crompton, A. W. (2003). Optimization of bone growth and remodeling in response to loading in tapered mammalian limbs. *Journal of Experimental Biology*, 206, 3125–3138.
- Lieberman, D. E., Polk, J. D., & Demes, B. (2004). Predicting long bone loading from cross-sectional geometry. *American Journal of Physical Anthropology*, 123, 156–171.
- Maggiano, I. S., Maggiano, C. M., Clement, J. G., Thomas, C. D., Carter, Y., & Cooper, D. M. (2016). Three-dimensional reconstruction of Haversian systems in human cortical bone using synchrotron radiation-based micro-CT: Morphology and quantification of branching and transverse connections across age. *Journal of Anatomy*, 228, 719–732.
- Main, R. P. (2007). Ontogenetic relationships between in vivo strain environment, bone histomorphometry and growth in the goat radius. *Journal of Anatomy*, 210, 272–293.
- Main, R. P., & Biewener, A. A. (2004). Ontogenetic patterns of limb loading, in vivo bone strains and growth in the goat radius. *Journal of Experimental Biology*, 207(Pt 15), 2577–2588.
- Martin, R. B., & Burr, D. B. (1989). *Structure, function and adaptation of compact bone* (pp. 275). New York: Raven Press.
- Martin, R. B., Burr, D. B., & Sharkey, N. A. (1998). *Skeletal tissue mechanics* (pp. 392). New York: Springer-Verlag.
- Martin, R. B., Gibson, V. A., Stover, S. M., Gibeling, J. C., & Griffin, L. V. (1996). Osteonal structure in the equine third metacarpus. *Bone*, 19, 165–171.
- Martiniaková, M., Grosskopf, B., Omelka, R., Vondráková, M., & Bauerová, M. (2006). Differences among species in compact bone tissue microstructure of mammalian skeleton: Use of a discriminant function analysis for species identification. *Journal - Forensic Science Society*, 51, 1235–1239.
- Mason, M. W., Skedros, J. G., & Bloebaum, R. D. (1995). Evidence of strain-mode-related cortical adaptation in the diaphysis of the horse radius. *Bone*, 17, 229–237.
- Mayya, A., Banerjee, A., & Rajesh, R. (2013). Mammalian cortical bone in tension is non-Haversian. *Science Reports*, 3, 2533.
- McFarlin, S. C., Terranova, C. J., Zihlman, A. L., & Bromage, T. G. (2016). Primary bone microanatomy records developmental aspects of life history in catarrhine primates. *Journal of Human Evolution*, 92, 60–79.
- Mears, C. S., Keenan, K. E., Kithas, A. A., & Skedros, J. G. (2014). Recognizing and resolving inconsistencies and inaccuracies in determining osteon circularity: Can methods be standardized? *American Journal of Physical Anthropology*, 153(S58), 183.
- Mears, C. S., Litton, S. M., Phippen, C. M., Langston, T. D., & Skedros, J. G. (2015). Improving accuracy, precision, and efficiency in analysis of osteon cross-sectional shape. *American Journal of Physical Anthropology*, 154(Suppl. 60), 223.
- Milgrom, C., Finestone, A., Simkin, A., Ekenman, I., Mendelson, S., Millgram, M., ... Burr, D. (2000). In-vivo strain measurements to evaluate the strengthening potential of exercises on the tibial bone. *Journal of Bone and Joint Surgery. British Volume*, 82, 591–594.
- Miskiewicz, J. J. (2016). Investigating histomorphometric relationships at the human femoral midshaft in a biomechanical context. *Journal of Bone and Mineral Metabolism*, 34, 179–192.
- Mohsin, S., O'Brien, F. J., & Lee, T. C., (2006). Osteonal crack barriers in ovine compact bone. *Journal of Anatomy*, 208, 81–89.
- Moreno, C. A., Main, R. P., & Biewener, A. A. (2008). Variability in forelimb bone strains during non-steady locomotor activities in goats. *Journal of Experimental Biology*, 211(Pt 7), 1148–1162.

- Moyle, D. D., & Bowden, R. W. (1984). Fracture of human femoral bone. *Journal of Biomechanics*, 17, 203–213.
- Moyle, D. D., Welborn, J. W. III., & Cooke, F. W. (1978). Work to fracture of canine femoral bone. *Journal of Biomechanics*, 11, 435–440.
- Mulhern, D. M., & Ubelaker, D. H. (2012). Differentiating human from nonhuman bone microstructure. In: C. Crowder, & S. Stout (Eds.), *Bone histology: An anthropological perspective* (pp. 109–134). Boca Raton, Florida: CRC Press.
- Mulhern, D. M., & Van Gerven, D. P. (1997). Patterns of femoral bone remodeling dynamics in a Medieval Nubian population. *American Journal of Physical Anthropology*, 104, 133–146.
- Paine, R. R., & Godfrey, L. R. (1997). The scaling of skeletal microanatomy in non-human primates. *Journal of Zoology London*, 241, 803–821.
- Paral, V., Witter, K., & Tonar, Z. (2007). Microscopic examination of ground sections - a simple method for distinguishing between bone and antler? *International Journal of Osteoarchaeology*, 17, 627–634.
- Parfitt, A. M. (1994). Osteonal and hemi-osteonal remodeling: The spatial and temporal framework for signal traffic in adult human bone. *Journal of Cellular Biochemistry*, 55, 273–286.
- Peterman, M. M., Hamel, A. J., Cavanagh, P. R., Piazza, S. J., & Sharkey, N. A. (2001). In vitro modeling of human tibial strains during exercise in micro-gravity. *Journal of Biomechanics*, 34, 693–698.
- Petrýl, M., Hert, J., & Fiala, P. (1996). Spatial organization of Haversian bone in man. *Journal of Biomechanics*, 29, 161–169.
- Pfeiffer, S., Crowder, C., Harrington, L., & Brown, M. (2006). Secondary osteons and Haversian canal dimensions as behavioral indicators. *American Journal of Physical Anthropology*, 131, 460–468.
- Pidaparti, R. M. V., & Turner, C. H. (1997). Cancellous bone architecture: Advantages of nonorthogonal trabecular alignment under multidirectional loading. *Journal of Biomechanics*, 30, 979–983.
- Portigliatti, B. M., Bianco, P., Ascenzi, A., & Boyde, A. (1984). Collagen orientation in compact bone: II. Distribution of lamellae in the whole of the human femoral shaft with reference to its mechanical properties. *Metabolic Bone Disease and Related Research*, 5, 309–315.
- Qiu, S., Rao, D. S., Palnitkar, S., & Parfitt, A. M. (2010). Dependence of bone yield (volume of bone formed per unit of cement surface area) on resorption cavity size during osteonal remodeling in human rib: Implications for osteoblast function and the pathogenesis of age-related bone loss. *Journal of Bone and Mineral Research*, 25, 423–430.
- Rasband, W. (1997–2016). *ImageJ*. 1.49v ed. Bethesda, Maryland: U.S. National Institutes of Health.
- Riggs, C. M., Lanyon, L. E., & Boyde, A. (1993a). Functional associations between collagen fibre orientation and locomotor strain direction in cortical bone of the equine radius. *Anatomy and Embryology*, 187, 231–238.
- Riggs, C. M., Vaughan, L. E., Boyde, A., & Lanyon, L. E. (1993b). Mechanical implications of collagen fibre orientation in cortical bone of the equine radius. *Anatomy and Embryology*, 187, 239–248.
- Rubin, C. T., Gross, T. S., Qin, Y., Fritton, S. P., Guilak, F., & McLeod, K. J. (1996). Differentiation of the bone-tissue remodeling response to axial and torsional loading in the turkey ulna. *Journal of Bone and Joint Surgery. American Volume*, 78, 1523–1533.
- Rubin, C. T., & Lanyon, L. E. (1984). Dynamic strain similarity in vertebrates; an alternative to allometric limb bone scaling. *Journal of Theoretical Biology*, 107, 321–327.
- Rubin, C. T., & Lanyon, L. E. (1985). Regulation of bone mass by mechanical strain magnitude. *Calcified Tissue International*, 37, 411–417.
- Rubin, C. T., Seeherman, H., Qin, Y. X., & Gross, T. S. (2013). The mechanical consequences of load bearing in the equine third metacarpal across speed and gait: The nonuniform distributions of normal strain, shear strain, and strain energy density. *FASEB Journal*, 27, 1887–1894.
- Ruff, C., Holt, B., & Trinkaus, E. (2006). Who's afraid of the big bad Wolff?: "Wolff's law" and bone functional adaptation. *American Journal of Physical Anthropology*, 129, 484–498.
- Schaffler, M. B., & Burr, D. B. (1984). Primate cortical bone microstructure: Relationship to locomotion. *American Journal of Physical Anthropology*, 65, 191–197.
- Sinclair, K. D., Farnsworth, R. W., Pham, T. X., Knight, A. N., Bloebaum, R. D., & Skedros, J. G. (2013). The artiodactyl calcaneus as a potential 'control bone' cautions against simple interpretations of trabecular bone adaptation in the anthropoid femoral neck. *Journal of Human Evolution*, 64, 366–379.
- Skedros, J. G. (2000). Do BMUs adapt osteon cross-sectional shape for habitual tension vs. compression loading. *Journal of Bone and Mineral Research*, 15 (Suppl 1), S347.
- Skedros, J. G. (2002). Use of predominant collagen fiber orientation for interpreting cortical bone loading history: Bending vs. torsion. *Journal of Bone and Mineral Research*, 17(suppl 1), S307.
- Skedros, J. G. (2012). Interpreting load history in limb-bone diaphyses: Important considerations and their biomechanical foundations. In C. Crowder & S. Stout (Eds.), *Bone histology: An anthropological perspective* (1 ed., pp. 153–220), Boca Raton, Florida: CRC Press.
- Skedros, J. G. (2014). Load complexity categories: An important consideration in bone adaptation studies. 7th World Congress of Biomechanics. Abstract retrieved from <http://teambone.com/wp-content/uploads/2014/2009/2111-Skedros-JG-Load-complexity-Categories.pdf>.
- Skedros, J. G., & Baucom, S. L. (2007). Mathematical analysis of trabecular 'trajectories' in apparent trajectorial structures: the unfortunate historical emphasis on the human proximal femur. *Journal of Theoretical Biology*, 244, 15–45.
- Skedros, J. G., Beckstrom, A. B., Kiser, C. J., & Bloebaum, R. D. (2008). The importance of bipedality/bending in mediating morphological adaptation in the chimpanzee femoral neck might be overstated. *American Journal of Physical Anthropology*, 46, 195.
- Skedros, J. G., Dayton, M. R., Sybrowsky, C. L., Bloebaum, R. D., & Bachus, K. (2006). The influence of collagen fiber orientation and other histocompositional characteristics on the mechanical properties of equine cortical bone. *Journal of Experimental Biology*, 209, 3025–3042.
- Skedros, J. G., Demes, B., & Judex, S. (2003a). Limitations in the use of predominant collagen fiber orientation for inferring loading history in cortical bone. *American Journal of Physical Anthropology*, 36, 193.
- Skedros, J. G., Hughes, P. E., Nelson, K., & Winet, H. (1999). Collagen fiber orientation in the proximal femur: challenging Wolff's tension/compression interpretation. *Journal of Bone and Mineral Research*, 14 (Suppl 1), S441.
- Skedros, J. G., & Hunt, K. J. (2004). Does the degree of laminarity mediate site-specific differences in collagen fiber orientation in primary bone? An evaluation in the turkey ulna diaphysis. *Journal of Anatomy*, 205, 121–134.
- Skedros, J. G., Hunt, K. J., & Bloebaum, R. D. (2004). Relationships of loading history and structural and material characteristics of bone: development of the mule deer calcaneus. *Journal of Morphology*, 259, 281–307.
- Skedros, J. G., & Keenan, K. E. (2016). Patterns of collagen fiber orientation in the human fibula middle-to-proximal diaphysis suggest a history of anterior-posterior bending and torsion consistent with

- "intermediate complexity" loading. *American Journal of Physical Anthropology*, 159(S62), 293.
- Skedros, J. G., Keenan, K. E., Cooper, D. M., & Bloebaum, R. D. (2014a). Histocompositional organization and toughening mechanisms in antler. *Journal of Structural Biology*, 187, 129–148.
- Skedros, J. G., Keenan, K. E., Halley, J. A., Knight, A. N., & Bloebaum, R. D. (2012). Osteon morphotypes and predominant collagen fiber orientation are adaptations for habitual medial-lateral bending in the human proximal diaphysis: implications for understanding the etiology of atypical fractures. *58th Annual Meeting of the Orthopaedic Research Society* (Vol. 37, pp. 1512), San Francisco, California, U.S.A.
- Skedros, J. G., Keenan, K. E., Litton, S. M., Skedros, G. A., & Mears, C. S. (2014b). Current exclusion criteria for selecting osteons for circularity analysis are potentially problematic. *American Journal of Physical Anthropology*, 153 (S58), 241.
- Skedros, J. G., Keenan, K. E., Mears, C. S., & Langston, T. D. (2015). The "shear resistance-priority hypothesis": A means for enhancing understanding of material adaptations in bones that habitually experience complex loading. *American Journal of Physical Anthropology*, 154 (Suppl. 60), 290.
- Skedros, J. G., Keenan, K. E., Williams, T. J., & Kiser, C. J. (2013a). Secondary osteon size and collagen/lamellar organization ("osteon morphotypes") are not coupled, but potentially adapt independently for local strain mode or magnitude. *Journal of Structural Biology*, 181, 95–107.
- Skedros, J. G., Kiser, C. J., Keenan, K. E., & Thomas, S. C. (2011a). Analysis of osteon morphotype scoring schemes for interpreting load history: Evaluation in the chimpanzee femur. *Journal of Anatomy*, 218, 480–499.
- Skedros, J. G., Kiser, C. J., & Mendenhall, S. D. (2011b). A weighted osteon morphotype score out-performs regional osteon percent prevalence calculations for interpreting cortical bone adaptation. *American Journal of Physical Anthropology*, 144, 41–50.
- Skedros, J. G., Knight, A. N., Clark, G. C., Crowder, C. M., Dominguez, V. M., Qiu, S., . . . Hulse, B. I. (2013b). Scaling of Haversian canal surface area to secondary osteon bone volume in ribs and limb bones. *American Journal of Physical Anthropology*, 151, 230–244.
- Skedros, J. G., Mason, M. W., & Bloebaum, R. D. (1994). Differences in osteonal micromorphology between tensile and compressive cortices of a bending skeletal system: Indications of potential strain-specific differences in bone microstructure. *Anatomical Record*, 239, 405–413.
- Skedros, J. G., Mason, M. W., & Bloebaum, R. D. (2001). Modeling and remodeling in a developing artiodactyl calcaneus: A model for evaluating Frost's mechanostat hypothesis and its corollaries. *Anatomical Record*, 263, 167–185.
- Skedros, J. G., Mason, M. W., Nelson, M. C., & Bloebaum, R. D. (1996). Evidence of structural and material adaptation to specific strain features in cortical bone. *Anatomical Record*, 246, 47–63.
- Skedros, J. G., Mendenhall, S. D., Kiser, C. J., & Winet, H. (2009). Interpreting cortical bone adaptation and load history by quantifying osteon morphotypes in circularly polarized light images. *Bone*, 44, 392–403.
- Skedros, J. G., Sorenson, S. M., Hunt, K. J., & Holyoak, J. D. (2007a). Ontogenetic structural and material variations in ovine calcanei: A model for interpreting bone adaptation. *Anatomical Record*, 290, 284–300.
- Skedros, J. G., Sorenson, S. M., & Jenson, N. H. (2007b). Are distributions of secondary osteon variants useful for interpreting load history in mammalian bones? *Cells Tissues Organs*, 185, 285–307.
- Skedros, J. G., Sybrowsky, C. L., Anderson, W. E., & Chow, F. (2011c). Relationships between in vivo microdamage and the remarkable regional material and strain heterogeneity of cortical bone of adult deer, elk, sheep and horse calcanei. *Journal of Anatomy*, 219, 722–733.
- Skedros, J. G., Sybrowsky, C. L., Parry, T. R., & Bloebaum, R. D. (2003b). Regional differences in cortical bone organization and microdamage prevalence in Rocky Mountain mule deer. *Anatomical Record*, 274A, 837–850.
- Sorenson, S. M., Jenson, N. H., & Skedros, J. G. (2004). Prevalence of atypical osteon characteristics may reflect adaptations in bending environments and during growth. *Journal of Bone and Mineral Research*, 19, S223.
- Starck, J. M., & Chinsamy, A. (2002). Bone microstructure and developmental plasticity in birds and other dinosaurs. *Journal of Morphology*, 254, 232–246.
- StataCorp. (2015). *Stata 14.1*. College Station, TX: StataCorp LP.
- Stoddard, G. J. (2016). *Statistical Issues in Basic Science: Robustness of the t-test even with small sample sizes. Biostatistics and Epidemiology Using Stata: A Course Manual*. Salt Lake City, Utah: University of Utah School of Medicine. Abstract retrieved from http://medicine.utah.edu/ccts/sdbc/resources/library.php#sdbc_library_stoddard_link.
- Stout, S. D., & Paine, R. R. (1992). Brief communication: Histological age estimation using rib and clavicle. *American Journal of Physical Anthropology*, 87, 111–115.
- Stover, S. M., Pool, R. R., Martin, R. B., & Morgan, J. P. (1992). Histological features of the dorsal cortex of the third metacarpal bone mid-diaphysis during postnatal growth in thoroughbred horses. *Journal of Anatomy*, 181, 455–469.
- Streeter, M., Stout, S., Trinkaus, E., & Burr, D. (2010). Brief communication: Bone remodeling rates in Pleistocene humans are not slower than the rates observed in modern populations: A reexamination of Abbott et al. (1996). *American Journal of Physical Anthropology*, 141, 315–318.
- Su, S. C., Skedros, J. G., Bachus, K. N., & Bloebaum, R. D. (1999). Loading conditions and cortical bone construction of an artiodactyl calcaneus. *Journal of Experimental Biology*, 202 Pt 22, 3239–3254.
- Swartz, S. M., Bennett, M. B., & Carrier, D. R. (1992). Wing bone stresses in free flying bats and the evolution of skeletal design for flight. *Nature*, 359, 726–729.
- Szivek, J. A., Johnson, E. M., & Magee, F. P. (1992). In vivo strain analysis of the greyhound femoral diaphysis. *Journal of Investigative Surgery*, 5, 91–108.
- Tersigni, M. A., Michael, A., & Byrd, J. E. (2008). Osteon area and circularity: a method for the assessment for human and non-human fragmentary remains. *Proceedings of the American Academy of Forensic Sciences* p 375, abstract H129, Washington, D.C., U.S.A.
- Tersigni-Tarrant, M. A., Byrd, J. E., & Manabe, J. (2011). Test of osteon circularity as a method of human/non-human identification. *Proceedings of the American Academy of Forensic Sciences*. p 381, abstract H090, Chicago, Illinois, U.S.A.
- Thomas, K. A., Harris, M. B., Willis, M. C., Lu, Y., & MacEwen, G. D. (1995). The effects of the interosseous membrane and partial fibulectomy on loading of the tibia: A biomechanical study. *Orthopedics*, 18, 373–383.
- Turner, C. H. (1998). Three rules for bone adaptation to mechanical stimuli. *Bone*, 23, 399–407.
- Urbanová, P., & Novotný, V. (2005). Distinguishing between human and non-human bones: Histometric method for forensic anthropology. *Anthropologie*, XLIII, 77–85.
- van Oers, R. F., Ruimerman, R., van Rietbergen, B., Hilbers, P. A., & Huiskes, R. (2008). Relating osteon diameter to strain. *Bone*, 43, 476–482.
- Warshaw, J. (2007). *Primate bone microstructural variability: Relationships to life history, mechanical adaptation and phylogeny* (pp. 1–440) [Doctor Of Philosophy, dissertation]. New York: The City University of New York.

- Warshaw, J. (2008). *Comparative primate bone microstructure: records of life history, function, and phylogeny* (pp. 385–425). In E Sargis & M. Dagosto M (Eds.), *Mammalian Evolutionary Morphology*: Springer Netherlands.
- Weaver, D. J., & Skedros, J. G., (2016). Do disparities in ex vivo strain data for the human fibula reflect heterogeneous load conditions or limitations of experimental designs? *American Journal of Physical Anthropology*, 159(S62), 331.
- Yeni, Y. N., Brown, C. U., Wang, Z., & Norman, T. L. (1997). The influence of bone morphology on fracture toughness of the human femur and tibia. *Bone*, 21, 453–459.
- Zedda, M., Lepore, G., Biggio, G. P., Gadau, S., Mura, E., & Farina, V. (2015). Morphology, morphometry and spatial distribution of secondary osteons in equine femur. *Anatomia, Histologia, Embryologia*, 44, 328–332.

How to cite this article: Keenan KE, Mears CS, and Skedros JG. Utility of osteon circularity for determining species and interpreting load history in primates and nonprimates. *Am J Phys Anthropol*. 2017;162:657–681. doi:10.1002/ajpa.23154.